Linnæus University
Sweden

Master's Degree Project

Wet spinning of carbon fiber precursors from cellulose-lignin blends in a cold NaOH(aq) solvent system

Author: Alice Landmér
Supervisor: Jan Brandin
Examiner: Michael Strand
External Supervisor: Andreas Bengtsson, Maria Sedin
Course Code: 4BT04E, 30 credits
Subject: Bioenergy technology
Level: Advanced
Department of Built Environment and Energy Technology

Linnæus University
Sweden

Abstract

Carbon fiber (CF) is predominantly produced from fossil-based sources and is therefore an area of interest for further development towards a more sustainable society. The purpose of this thesis work was to investigate the possibility of producing precursor fibers (PFs) for CF production from a blend of renewable cellulose and lignin. Cellulose, which is used to some extent for CF production, was chosen, while the possibility of adding lignin was investigated in hope of increasing the gravimetric yield of the CF production.

Blends of softwood kraft cellulose pulp (SKP) and softwood kraft lignin (SKL) were dissolved in an alkaline (NaOH) solvent system at different cellulose/lignin ratios. A total of eight dopes were prepared (SKP/SKL ratios of 100/0–60/40 wt./wt.) with total dope concentrations ranging from 4.5 wt.% to 9.2 wt.%. The addition of SKL resulted in dark colored dopes with viscosities of which mainly appeared to depend on the SKP concentration.

The dopes were wet spun, resulting in continuously spun PFs. The PFs showed on an increasing pyrolysis yield with increased SKL content but decreasing mechanical properties. However, process optimization was not included in the work, subsequently leading to the assumption that greater values on mechanical properties can be achieved.

A pure SKP PF and a SKP-SKL (70/30 wt./wt.) PF were successfully thermally converted into CFs by carbonization at 1000 °C. The PF containing SKL had a total gravimetric yield more than twice as high as the pure SKP PF, 28 wt.% and 12 wt.%, respectively. Thereby, the addition of SKL seems to have a positive impact on the CF yield when utilizing a $NaOH_{(aq)}$ solvent system.

This thesis work has become a base for the future work towards the development of CFs from wet spun cellulose-lignin PFs in the NaOH(aq) solvent system.

Keywords

Carbon fiber, cellulose, cold NaOH(aq), lignin, precursor, sodium hydroxide, solution spinning, wet spinning

Acknowledgments

This master thesis project would not have been possible without the help and support from some kind souls. Thereby, I acknowledge, with respect and admiration, the following:

My supervisor Maria Sedin who gave me the opportunity to be a part of this project and has supported me through the whole thesis work with ideas and good advise, while sharing the excitement of the research work and its outcomes.

My supervisor and spinning partner Andreas Bengtsson who has had patience, shared great knowledge as well as advise regarding the work with fibers, while always spreading the joy of science.

The people at RISE Bioeconomy and Health in Stockholm: Lars Norberg for support and guidance with good advise in the lab, and Elisabeth Bränvall for inputs regarding pulp questions and previous spinning trails.

Linnaeus university for the support in choosing a thesis subject of my liking.

My wonderful partner Harald for taking care of our home and making sure I had a place to stay at in Stockholm, as well as providing me with positive energy and enabling me to focus on my thesis work.

Table of contents

1 Introduction **1**
1.1 Objective *2*

2 Background **3**
2.1 Wood components *3*
2.1.1 Cellulose 3
2.1.2 Lignin 5
2.2 Solvent systems *7*
2.2.1 Ionic liquids (ILs) 8
2.2.2 Cold NaOH(aq) 9
2.3 Solution spinning *11*
2.4 Processes for cellulose fiber production *13*
2.4.1 The Viscose process 13
2.4.2 The Lyocell process 14
2.5 Carbon fibers *15*

3 Materials and methods **17**
3.1 Materials *17*
3.2 Cellulose-lignin dope preparation *17*
3.3 Precursor fiber preparation *18*
3.4 Preparation of carbon fibers *19*
3.5 Characterization *19*
3.5.1 Dope stability 19
3.5.2 Dope viscosity 19
3.5.3 Fiber morphology 20
3.5.4 Pyrolysis yield 20
3.5.5 Tensile properties 20
3.5.6 Ash content 20
3.5.7 Ash composition 20

4 Results and discussion **21**
4.1 Dope preparation and stability *21*
4.2 Precursor fibers *23*
4.2.1 Wet spinning trials 23
4.2.2 Morphology of precursor fibers 25
4.2.3 Ash content of precursor fibers 26
4.2.4 Tensile properties of precursor fibers 28
4.2.5 Pyrolysis yield of precursor fibers 30
4.3 Conversion to carbon fiber *32*

5 Conclusions **36**

6 Future work **37**

References **38**

Appendices

Appendix 1 – Spinning dopes

Appendix 2 – Spinning settings

Appendix 3 – Ash content of precursor fibers

Appendix 4 – Mechanical properties of precursor fibers

Appendix 5 – Pyrolysis yield of precursor fibers

List of Abbreviations

AGU	anhydroglucossidic unit
BSE	backscattering electron
CF	carbon fiber
DESs	deep eutectic-based solvents
D.I.	deionized
DP	degree of polymerization
DS	dry solid
EDXA	energy dispersive X-ray analysis
IL	ionic liquid
KL	kraft lignin
NMMO	*N*-methylmorpholine *N*-oxyde
PAN	polyacrylonitrile
PEG	polyethylene glycol
PF	precursor fiber
RH	relative humidity
RTILs	room-temperature ionic liquids
SEM	scanning electron microscope
SKL	softwood kraft lignin
SKP	softwood kraft pulp
TGA	thermogravimetric analysis
TM	tensile modulus
TS	tensile strength

1 Introduction

Due to an evolving and expanding society there have emerged a simultaneous increase of environmental concerns as well as a demand of new materials and products. Hence, a need of developing more sustainable processes to protect the Earth's wealth and resources has arisen. The need to decrease the world's dependence on petrochemicals is one of the matters that must be tackled, e.g., by development of processes using renewable raw materials. Thereby, the utilization of resources from the forestry has become a cornerstone in the development and the progress towards a sustainable economy.

Carbon fiber (CF) is a lightweight material with several valuable characteristics making it desirable as a load-bearing component in composites. With the beneficial tensile properties of high specific strength and stiffness, CF is attractive in e.g., structural and transport applications. Commonly used precursor for the production of CFs are predominantly the fossil-based polyacrylonitrile (PAN) which is used for roughly 96 % of the CFs, while the rest are being produced from either rayon (regenerated cellulose) or petroleum pitch [1]. In addition to cellulose, the forestry is also a source of lignin. The potential of using the carbon rich lignin (60–65 %) [2] as a renewable CF precursor has been evaluated through a considerable amount of research. Kraft lignin, which is obtained from the kraft pulping process can be processed into precursor fibers (PFs) by melt spinning. However, there are still great challenges to overcome regarding the processing of these PFs into CF as well as the relatively low mechanical properties of these lignin-derived CFs. In contrast to the complex amorphous kraft lignin, cellulose is a linear polymer with molecular orientation, which is beneficial for the mechanical properties of the PF and CF. However, cellulose-based CFs are expensive to produce due to the relatively low carbon content (44.4 %) and a low CF yield (10–30 %) [3] [4]. Nevertheless, a mutual benefit for cellulose and lignin is the high availability of the materials around the globe.

By comparing benefits and drawbacks of lignin and cellulose as potential precursors for CF production, it could be suggested that a precursor made from a blend could lead to positive attributes for the purpose of CF production. The LightFibre project at RISE (Research Institutes of Sweden) demonstrated that PFs and CFs from cellulose and kraft lignin blends have several advantages [5] [6] [7] [8]. Cellulose pulp and kraft lignin were co-dissolved in an ionic liquid (IL) and then dry-jet wet spun into PFs. The cellulose made the PF flexible and easy to handle, and the wet spinning technique contributed to the possibility to bypass many of the technical challenges encountered in conjunction with melt spinning of kraft lignin (e.g., the need of fractionation steps to obtain low molecular weight lignin and the long stabilization time needed during conversion to CF). In addition, the mechanical properties of the obtained CFs from the Lightfibre project are promising. However, using ILs for the dissolution of the raw materials is expensive, as it is no commercially available recycling process, and therefore its replacement with a cheaper solvent is the prime motivation of this thesis.

1.1 Objective

The aim of this thesis was to investigate the possibility of producing a precursor fiber (PF) for carbon fiber (CF) production through wet spinning of a softwood kraft cellulose pulp (SKP) and softwood kraft lignin (SKL) blend in a cold NaOH(aq) solvent system.

The objective was to first investigate if homogenous spin dopes of SKP and SKL blends could be prepared in the devised system, and if the dopes were spinnable. Thereafter, the influence of total dope concentration and SKP/SKL blend ratios on the dope stability and spinnability in the system was investigated. In addition, the effect of the SKL addition on the pyrolysis yield was investigated based on the blend ratios as well as the ash content of PFs depending on wash bath retention time. The blend ratios were extensively studied, while the spinning settings were held constant throughout the work. Emphasis was placed on spinnability, PF tensile properties and pyrolysis yield.

2 Background

2.1 Wood components

The main components in wood are cellulose, hemicellulose (e.g., glucomannan, xylan) and lignin, which are accompanied by a minor fraction of extractives (0.3–4.8 %) [9]. Cellulose generates the skeletal matrix of wood which is surrounded by hemicellulose, and lignin that fills up the space and fixates the different components towards each other (Fig. 1) [10].

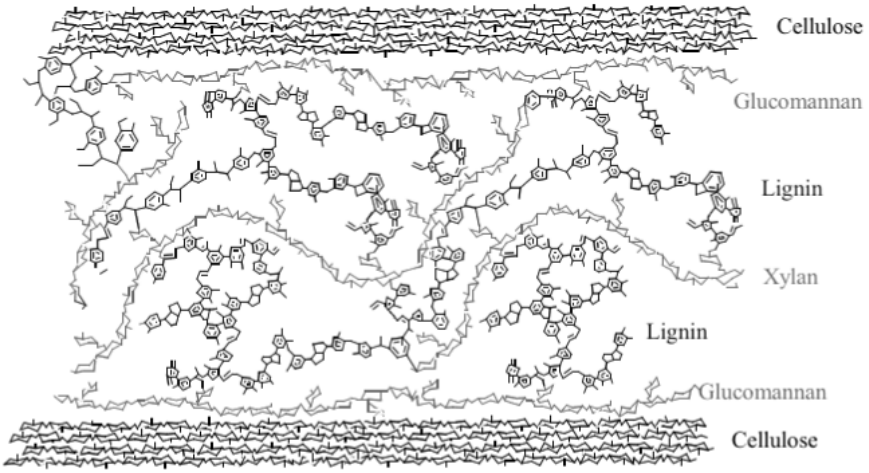

Figure 1. Wood components at a molecular level [11].

However, the composition and fraction of each constituent depends on the wood source (Tab. 1).

Table 1. Chemical composition in different types of wood [12].

Type of wood	Cellulose (%)	Hemicellulose (%)	Lignin (%)
Temperate softwood	40–45	25–30	25–30
Temperate hardwood	40–45	30–35	20–25
Eucalypt	45	20	30

2.1.1 Cellulose

Cellulose is the most abundant biopolymer in the world, and is a semicrystalline linear polymer built up by D-glucopyranose units, also called anhydroglucosidic units (AGU) [13] [14]. The degree of polymerization (DP) is often high in its native state, cellulose I, and in wood the cellulose consists of about 10,000 AGUs [10].

In wood the cellulose is found in the multiple cell wall layers as fibers, which are built up by fibrils that are assembled from microfibrils, consisting of both crystalline and amorphous regions. The microfibrils, in turn, originates from bundles of cellulose molecules that have aggregated together, where the less ordered (amorphous) regions within the molecule structure occurs due to a kink at every 6–7 AGU [14]. The AGUs

in the molecule are linked together through a β-1→4 glycosidic bond creating a chain, where every AGU is displaced 180° with respect to its neighboring units (Fig. 2), which results in a 2-fold screw axis [10]. Each AGU in cellulose has three equatorially positioned hydroxyl groups (located at C2, C3, and C6) between which intra- and intermolecular hydrogen bond formation occurs [10] [14]. The hydrogen bond formation between the hydroxyls at C6 and C3 of neighboring chains lead to a parallel arrangement of the chains which forms a sheet. Several sheets are then stacked over each other and linked through van der Waals bonds and hydrophobic interactions [13].

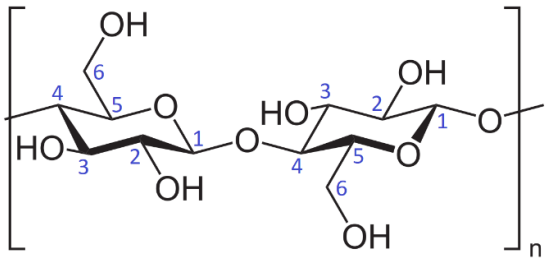

Figure 2. The molecular structure of cellulose.

A crystalline microfibrillar structure is formed due to the cellulose sheet interactions, and occurs in two different varieties, Iα and Iβ, in nature. The difference lay in the hydrogen-bonding and sheet stacking patterns of the cellulose [13]. The meta-stable Iα is dominant in native wood and is almost three times as high as the Iβ content. However, at high temperature and pressure in an acidic or alkaline solution the Iα can be transformed into the more stable Iβ. This is for example achieved during the kraft pulping process where it has been shown, for spruce wood, to shift into a distribution where the Iβ content is roughly twice as high as the Iα [15]. Additionally, during the kraft pulping process another configuration of cellulose will form, cellulose II, which will be present alongside the native cellulose (cellulose I) in the pulp [16].

Cellulose II is the more thermodynamically stable version of cellulose, and is thought to have anti-parallel oriented chains in contrast to cellulose I. Cellulose II is one of the three known and most common crystalline structures which can be obtained through thermal and chemical treatments of cellulose I. To generate cellulose II, the structure of cellulose I is modified by treatment with alkali (mercerization) or by being dissolved and regenerated. [13] [17]

Dissolution of cellulose

The dissolution of cellulose occurs in two stages, 1) swelling (intercrystalline and/or intracrystalline), and then 2) breakage of the polymer-polymer intermolecular forces, i.e., hydrogen bonding [18]. Many solvents can achieve the first stage, but few will achieve the second, which result in an insolubility of cellulose in most solvents. It is suggested by *E. Sjöström* (among others) that the fibrous structure and strong hydrogen bonds are thought to be the reason for its insolubility in most solvents [10].

To enable complete dissolution of cellulose the solvent used has to be able to penetrate into each of the cell wall layers as well as break all the attractive forces between the chains [14]. Cellulose is an amphiphilic polymer, i.e., it has both polar and nonpolar regions, but it has a relatively polar nature with its several hyrdoxyl

groups. The geometrical position of these polar and nonpolar regions strongly affects the solubility. Cellulose is insoluble in nonpolar organic solvents, but more surprisingly also in water, which commonly is suggested to be a result of the intra- and intermolecular hydrogen bonds. However, the aqueous insolubility is difficult to understand, and research is still carried out on the topic in search of an improved understanding. Nevertheless, there are some solvents that can dissolve cellulose e.g., the amphilic solvents *N*-methylmorpholine *N*-oxyde (NMMO)/water and ionic liquids (ILs), as well as phosphoric acid-based solvents, NaOH-water, LiCl-based solvents, and some others [17]. The use of co-solvents with the tendency to weaken hydrophobic interactions, such as urea and polyethylene glycol (PEG), has shown to promote the aqueous solubility of cellulose. [19]

However, there are measures that can be made to aid the dissolution of cellulose, and pre-treatments and processing are essential to increase the capability of dissolving wood cellulose. One measure is to decrease the DP of the cellulose chains as a high DP, like in the wood cellulose native state, obstructs dissolution. A pulping process will not only separate the cellulose but also decrease the DP to 300–1700 depending on process [14], where pulp in the lower range (DP 250 to 600) typically is referred to as dissolving grade pulp. Another measure to increase the solubility could be to introduce charges to the cellulose, e.g., by adding functionalizing groups or conducting deprotonation [20].

2.1.2 Lignin

Lignin is a complex macromolecule built up of phenylpropane units. Many features of the lignins native structures are still unclear, e.g., the molecular weight, as it is impossible to determine this due to the lignins close association with the wood polysaccharides. The lignin structure is built up by a three-dimensional web where the monomers, also called monolignols, are connected with randomly distributed ether (C-O-C) and carbon-carbon (C-C) bonds. There are three main monolignols from which lignins are polymerized, namely *p*-coumaryl alcohol, coniferyl alcohol and sinapyl alcohol (Fig. 3), but there are also other more unusual monolignols.

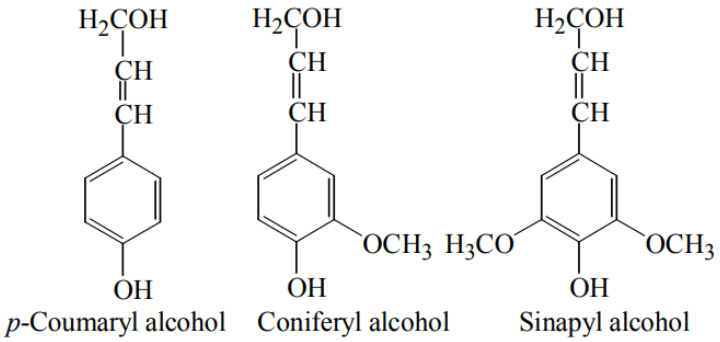

Figure 3. The three main monolignols [11].

The distribution ratio of the different monolignols differs significantly depending on the source of the lignin (Tab. 2), and thereof the lignin has no general repeated structure common for all lignins. However, the types and different amounts of each bond within the various lignins have been thoroughly investigated and determined. [10] [11]

Table 2. Distribution of monolignols depending on source [11].

Plant	p-Coumaryl alcohol (%)	Coniferyl alcohol (%)	Sinapyl alcohol (%)
Coniferous (softwoods)	<5	>95	None or Trace
Eudocotyledonous (hardwoods)	0–8	25–50	46–75
Monocotyledonous (grasses)	5–33	33–80	20–54

The monolignols in the aromatic ring are numbered 1 to 6, and the aliphatic carbons in the propyl chain attached at C1 are named α, β and γ starting from the carbon closest to the ring. Most commonly occurring bonds in lignin are four types of C-C bonds and three types of ether linkages. The dominant bond in both hardwood and softwood lignin is the β-O-4' bond. In native lignin only 10–13 % of the oxygen atoms at position C4 do not form an ether bond, which result in free phenolic hydroxyl groups. The β-O-4' bond is the main bond degraded during delignification in the kraft pulping process. The ratio of monolignols with a free C5 position (absence of the methoxyl group) is higher in softwood lignins, compared to hardwood lignins. Consequently, the degree of condensed bonds such as β–5' or 5–5' are higher in softwood, subsequently leading to a more branched molecule which is more eager to react upon e.g., thermal treatment. [11]

However, it should be noted that the lignin structure not only depends on the wood species, but also on the pulping conditions and/or isolation method used. Therefore, the focus will solely be kept on kraft lignin in further parts of this report.

Dissolution of kraft lignin

Kraft lignin (KL) has no or low solubility in most of the common and traditionally used solvents. However, KL is soluble in some solvents with acidic and basic character, organic-based and IL-based systems [21]. The phenolic content of KL is important for its degree of reactivity [11], and with a decreasing molecular mass the phenolic group content per monomer will increase [22]. Additionally, a decrease in molecular mass will also lead to a higher degree of disentanglement which increases the solubility of the KL [23]. However, the bonds between the monolignols in KL are relatively stable – with the exception of the α-O-4 bond – but the C-C bonds, which are the most resistant bonds, often survives the chemical pulping process [11].

The possibility to dissolve KL in solvents, having either acidic or basic character, indicates the important role of protonation and deprotonation for the dissolution of KL. The organically bound sulfur of KL, present as a thiol group (pKa 11.6 [24]), becomes deprotonated at alkaline pH (~10) and the molecule becomes more polar, enabling it to dissolve. The introduction of charges on the polymer chain, with the

help of extreme pH, increases the solubility of KL, an effect similar to what have been observed for polymers, e.g., cellulose. Some areas of the KL seem to obtain distinct polarity and are therefore expected to have some sort of amphiphilic behavior, and e.g., aggregate in an aqueous media [25]. As a result, it should be beneficial to weaken the hydrophobic interactions among the KL molecules, and the presence of surfactant-like molecules, e.g. sodium salts of bile acid, might stabilize the KL which has been shown to be able to re-disperse after being aggregated when adding these natural amphiphiles [26]. Research also supports the use of compounds with intermediate polarity, e.g., alcohols, ethylene glycol or γ-valerolactone, for efficient dissolution. [21]

It is believed, by e.g., *Melro et al.*, that a good solvent for the dissolution of KL should be capable of competing with both the hydrophobic interactions and the hydrogen bond network among the KL molecules [21].

2.2 Solvent systems

There are different types of solvents that can be used for the preparation of dopes which are to be utilized in solution spinning processes. The choice of solvent system greatly depends on the material which is to be dissolved.

The solvents used for dissolution of cellulose can be categorized by the distinction of being either derivatizing or non-derivatizing. Derivatizing solvents accomplish a derivatization, of e.g., the cellulose, prior to the dissolution whilst non-derivatizing ones could be seen as direct solvents [14].

Important solvents for the dissolution of cellulose into non-derivatized and non-complexed solutions are e.g., phosphoric acid-based solvents, lithium chloride-based (LiCl) solvents, NMMO, ILs and NaOH-water [27]. When using phosphoric acid as a solvent, the spinning of a concentrated cellulose-phosphoric acid solution can provide fibers with high tensile modulus and strength (TM 44 GPa, and TS 1.7 GPa) [28]. Utilization of non-aqueous solvents, such as the mixture of LiCl and NMMO, are common in methods for analysis of cellulose chains. However, these are not commercially applied for the purpose of producing cellulose materials [27]. On the other hand, NMMO mixed with water is used industrially to produce fibers (Lyocell process) which are primarily used within the textile industry [29].

In the review by *Melro et al.* it becomes clear that the KL solubility is enhanced in solvents of intermediate polarity, a behavior also identified in cellulose [21]. For example, the chain length of alcohols is an important factor for the possibility to dissolve KL, which has been suggested to be due to the hydrogen bonding capacity which will decrease as the length of the aliphatic hydrocarbon side chain increases [30]. The same trend, regarding chain length of solvent, is shown for carboxylic acids, where a higher dissolution of KL is achieved with formic acid than acetic acid or other with longer carbon chains [21]. The use of heterocyclic compounds, e.g., pyridine and 1-methylimidazole, have shown a high KL dissolution capacity (>500 g/kg [31]). However, the reported conditions to achieve full dissolution are not mild. Another solvent system suitable for dissolution of KL are the deep eutectic-based solvents (DESs), consisting of a mixture of a hydrogen bond acceptor and a hydrogen bond donor. The DESs are similar to ILs, however, DESs are often biodegradable and

generally much less expensive to synthesize and less toxic [21] [32] [33]. Additionally, the DESs have the advantage over traditional ILs as there is a possibility to incorporate water without affecting the KL dissolution performance [21].

The ILs and NaOH-water solvent systems, both with the capability to dissolve SKP and SKL, will be further described in section 2.2.1 and 2.2.2.

2.2.1 Ionic liquids (ILs)

ILs are liquids which consist of exclusively, or almost entirely, of ions, and therefore exhibit ionic conductivity. Hence, it should be noted that aqueous solutions of salts do not fulfil the criteria of being an IL. In the past two decades or so, the term IL has been limited to liquids following this definition above with the addition of also having a melting point or glass-transition temperature below 100 °C. Furthermore, a fledgling interest for room-temperature ionic liquids (RTILs), which are in liquid state at or around room temperature, have arised within the last few years. Liquids that fulfil these criteria are typically organic salts or eutectic mixtures of organic and inorganic salts. [34]

There are many various reasons for the extensive attraction of ILs, e.g., [34] [35]:

- There is an almost limitless number of possible IL systems, combinations of anions and cations, which can be tailored for specific purposes, e.g., by designing specific functionalities into the cations and/or anions, or by mixing two or more ILs.
- A negligible vapor pressure and do not evaporate under normal conditions.
- Generally non-flammable.
- Possess high thermal and electrochemical stability.
- Wide range of solubilities and miscibilities (e.g., hydrophilic, or hydrophobic).
- Can be used for separations and extractions of chemicals from both aqueous and molecular organic solvents.
- Theoretically easy to recycle after use as solvent and/or catalyst. Although, in industrial scale it will become an expensive process-step.

Initially ILs were seen and formulated as “green solvents” due to the advantages mentioned above, such as low vapor pressures, high stability and relatively non-toxicity [36]. However, this “green” label should not be generalized, as ILs still possess some important limitations (e.g., high price, poor biodegradability, questionable biocompatibility, and sustainability issues) which becomes an issue and is unappealing in large scale use at the moment [21].

An IL system is a possible alternative to organic solvent systems for the dissolution of KL, and both aprotic and protic systems have been investigated as possible candidates. The imidazolium based aprotic ILs have gained extensive attention as possible solvents for KL, and several have shown good capability to achieve a high

dissolution of KL [21]. Other investigated IL solvents for dissolution of KL are ammonium, phosphonium and pyrrolidinium based, which also show reasonable dissolution capabilities [37]. The dissolution of KL in ILs is still not fully understood, but observations have shown that both the anion and the cation play important roles. Additionally, even if some ILs can dissolve KL at room temperature an increased temperature will also increase the dissolution degree of the KL [21]. According to *Melro et al.* the protic ILs seem to achieve the highest degree of KL dissolution [21].

Some ILs have the potential of dissolving cellulose as non-derivatizing solvents, and have become attractive e.g., due to the advantages already mentioned. Furthermore, it has been shown that ILs can dissolve relatively high concentrations of cellulose, which is thought to be a result of the solvents strong hydrogen bonding to the polymer. The crucial role of the anion is widely stated in the literature, and chloride ions are reported to have a special effect on breaking hydrogen bonds. The dissolving capabilities of ILs are therefore widely attributed to polar-electrostatic interactions between the solvent ions and the hydroxyl groups of the cellulose. On the other hand, studies have also shown that it seems like several other anions work well, e.g., 1-ethyl-3-methyl-imidazolium acetate ([EMIM][OAc]) which molecular structure is shown in Fig. 4 [6]. However, other experimental studies support the importance of the cation, which requires a special structure, and it seems that an amphiphilic cation is required to facilitate dissolution of cellulose [19]. [35]

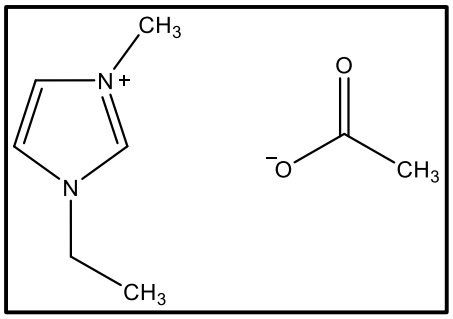

Figure 4. Structure of the IL [EMIM][OAc], which holds the ability to dissolute both SKP and SKL.

2.2.2 Cold NaOH(aq)

The aqueous NaOH systems are both easily prepared and have a low environmental pollution potential, hence becoming an interesting option as a solvent system [38]. Already during the 19th century the development of processes including cellulose and aqueous NaOH systems were completed, as John Mercer patented the mercerization process [39], while Cross and Bevan later patented the viscose process [40]. However, it was not until the early 20th century that the use of NaOH(aq) as a possible solvent for cellulose was discovered, which was patented by Lilienfeld in 1924 [41].

It has been reported that at specific conditions, the NaOH(aq) will be able to break the hydrogen bonding network of the cellulose [42] [43], which then enables the dissolution. Additionally, it has been suggested that the NaOH(aq) acts as a deprotonating agent [44], which in addition to hydrogen bond breakage also leads to the formation of a polyelectrolyte and the introduction of repulsive forces between the chains [14]. However, this has not yet been proven.

The preferable concentration of NaOH in an aqueous solution with the purpose of dissolving cellulose has been shown to be in the range of 7–10 wt.% (Tab. 3). On the other hand, for the dissolution of KL a 1 wt.% alkali aqueous solution is generally considered as a good solvent [21].

Table 3. Effect of the NaOH concentration in cellulose dope solutions at low temperatures [45].

Case	Temp. °C	NaOH conc.	Effect
Low	<0	<6–7 %	Do not count as a solvent since it does not dissolve the cellulose.
Preferable	<0	7–10 %	NaOH penetrate into the fibers and detach individual chains into the solution. No formation of Na/cellulose crystal.
High	<0	>18–20 %	The cellulose chains form Na/cellulose crystal formations (mercerization).

Egal et al. investigated the dissolution of cellulose in NaOH(aq) systems and determined the ratio limit of dissolution to be at least four NaOH molecules per AGU, or a cellulose/NaOH weight ratio of one [45]. If the concentration of cellulose where to be higher it would not dissolve. Thereby, within the preferred NaOH concentration range for solution, a maximum capacity of dissolving an amount of 10 % cellulose is given.

In addition to the concentrations, of NaOH and cellulose, the temperature of the system play an important role. It is generally stated that the temperature must be kept between -10 °C and +10 °C for the cellulose to remain dissolved in the NaOH(aq) solution. When NaOH is present in water an eutectic structure forms, giving a lower solidification temperature of the mixture, which decreases in quantity in the presence of cellulose [38] [46]. Additionally, a lower temperature is desirable as the network of NaOH hydrates increase in strength with a decreasing temperature, which probably is a result of the increasing strength of the hydrogen bonds [45]. Hence, at low temperatures, hydrates can penetrate into the cellulose structure and then create a network with themselves, rather than bind to the cellulose, and thereby prevent the dissolved cellulose chains from interacting with each other.

Additives can be used to improve the dissolution of cellulose in NaOH(aq), as well as to improve the stability of the solution (dope). Due to the narrow dissolution window combined with the relatively unstable nature of cellulose and its tendency to aggregate in NaOH(aq) systems, the use of additives becomes essential. A common additive used for the purpose to improve the dissolution is urea [47], which also is known to break hydrophobic interactions. Other examples of additives utilized for dissolution of cellulose in cold NaOH(aq) are e.g. thiourea [48], ZnO [49] and PEG [50]. [19]

The Q-state refers to a region between -5 and +1 °C for a 7 to 10 wt.% NaOH solution, marked with a red circle in Fig. 5. Within this narrow window, the dissolution of cellulose occurs in the cold NaOH(aq) system [42].

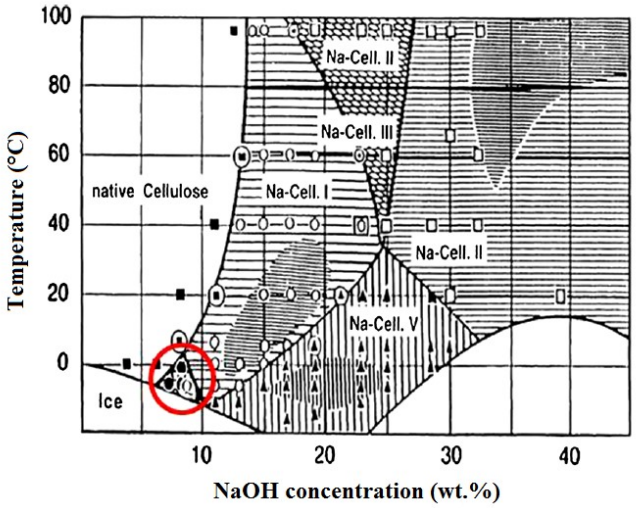

Figure 5. Phase diagram of cellulose-water-NaOH, adapted from Sobue [42].

The effect on dissolution when adding both cellulose and lignin to the same NaOH(aq) solution has been investigated by e.g., *Sescousse et al.* [51]. The authors obtained visually homogeneous mixtures, with no signs of phase separation within one week of storage time in a refrigerator, when using an 8 wt.% NaOH solution for the dissolution.

However, there is still a lack of understanding regarding the structure and properties for the cellulose/NaOH(aq) solutions. Additionally, the narrow process window for dissolution as well as the problems with incomplete dissolution when having high-DP cellulose are great challenges which needs to be tackled to enable and create a successful process using the NaOH(aq) solvent system.

2.3 Solution spinning

Solution spinning (collective term for wet spinning and dry-jet wet spinning) and melt spinning are commonly used techniques for the preparation of PFs for CF. The choice of technique is highly affected by the properties of the raw material which is to be processed. For instance, when conducting melt spinning the raw material require certain thermoplastic properties anticipating the material to melt before decomposition, but for materials such as PAN and cellulose which will decompose before melting, the solution spinning process becomes a necessity.

To be able to solution spin a material, it has to be a polymer which is soluble in a solvent from which it later can be regenerated. The material (polymer) is regenerated from the solution, i.e., the spinning dope, by using a coagulation liquid which extract the solvent from the dope. Hence, solvents such as ILs, acid-based or alkaline-based, etc. are suitable for the purpose.

The wet spinning process (Fig. 6) is generally built up by four main steps:

1. A dope is prepared out of the chosen raw material by dissolution in a suitable solvent system. The dope is placed in a tank/container connected to a pump which feeds the dope to a spinneret positioned in a coagulation bath.
2. The dope is extruded directly into the coagulation liquid where filaments solidify as the solvent in the dope diffuse out as an effect of the bath solution. The formed filaments are then collected in a tow.
3. The tow is led through wash bath(s) while being stretched. Impurities from the coagulation bath are removed while the stretching may induce uniaxial molecular orientation and diameter reduction of the filaments.
4. The filaments are dried and then collected on a winding bobbin. Different finishes can be applied in this step, either before or after drying, to obtain certain properties of the filaments (e.g., less friction, anti-static, anti-bacterial).

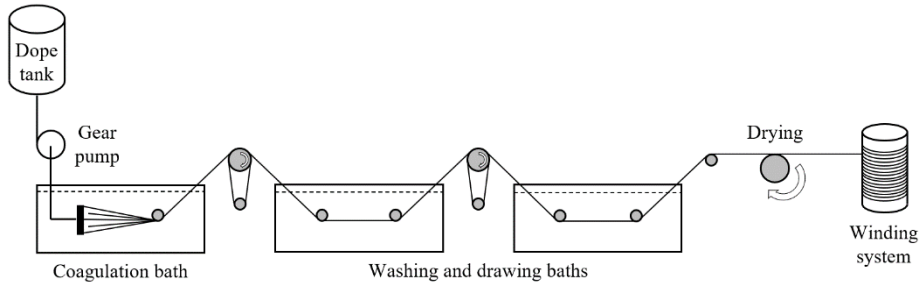

Figure 6. Schematic illustration of the wet spinning process.

To achieve a successful wet spinning it is highly important to have no undissolved particles and an fully deaerated dope. The latter is particularly important as air bubbles in the dope might lead to filament breakage if they pass through a hole in the spinneret. To obtain an industrially robust wet spinning process, a high degree of solvent recovery will be needed for economical and environmental reasons.

Dry-jet wet spinning is another solution spinning technique which is similar to the classical wet spinning. The main difference is the extrusion step of the process (step 2 above), where the spinneret is placed in the air above the coagulation bath instead of directly in the coagulation liquid, see Fig. 7. Benefits with dry-jet wet spinning are that a higher dope concentration can be used, thereby less solvent, and that high tensile strength and elongation properties can be obtained, a result of the enhanced molecular orientation induced by the draw in the air gap. Nevertheless, limitations with the dry-jet wet spinning technique are the relatively high dope viscosities required (which requires a more potent dope solvent, e.g., ILs) as well as the challenges with tuning the air flow usually used in the air gap. If the latter is too high, it may lead to neighboring filaments coming into contact and ultimately coagulate into a larger, combined, filament. [29]

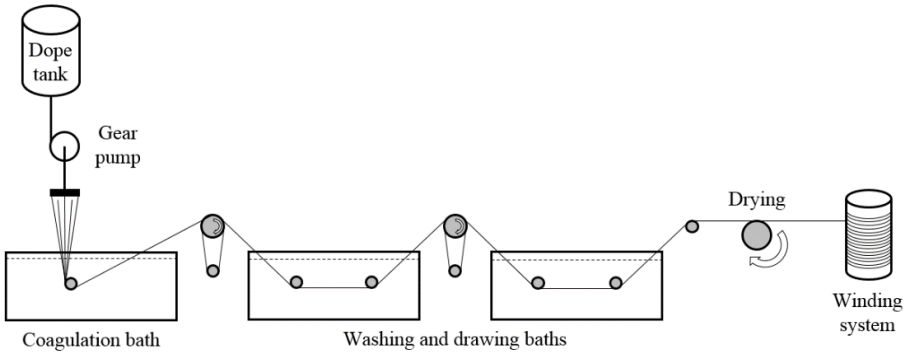

Figure 7. Schematic illustration of the dry-jet wet spinning process.

2.4 Processes for cellulose fiber production

Two well established fiber production processes using wood cellulose as raw material are the viscose process and the lyocell process, these will be briefly described below.

2.4.1 The Viscose process

In 1893 the first patent for the viscose process was granted to Cross and Bevan [40]. Since then, the process has undergone many modifications, but the basic chemistry remains the same. The process consists of a series of controlled steps where short fibered wood pulp (a variety of dissolving-grade pulps are used) is converted into a spinnable dope out of which longer filaments are spun to fulfil desired properties and design. The viscose process uses a derivatizing system and apply the wet spinning technique to produce fibers.

As raw material, a high-grade cellulose pulp is required, which generally is recovered from spruce or eucalyptus wood. The cellulose is usually separated from the wood source by the kraft or sulphite cooking process, which results in a pulp with a typical DP of 750 to 850. The pulp is pressed and cut into sheets which thereafter are slurried/swollen in NaOH(aq), forming alkali cellulose. Excess soda is pressed out allowing the solvent to be recovered and re-used in the slurry step. Pre-aging of the alkali cellulose is thereafter done, stored with access to air, leading to oxidization and reduction of the pulp DP to around 270 to 350. Pre-aging is highly important as it will affect the viscosity and thereby the spinnability of the dope. Then, the process step xanthation is carried out, a step where carbon disulphide (CS_2) is used to treat the alkali cellulose leading to the formation of sodium cellulose xanthate, an orange-colored viscous liquid. The sodium cellulose xanthate is thereafter dissolved in NaOH(aq) to form the viscose spinning dope. The dope is set to mature, which will improve the spinning qualities, while held under vacuum to remove air bubbles. After maturing, the dope is filtered to remove any particles and undissolved cellulose which could generate problems such as clogging of spinneret holes during spinning. Finally, the dope undergoes deaeration where any dispersed air or gas bubbles are removed from the dope. [10] [18] [40]

The viscose is extruded through a spinneret (generally ‘full-face’ or ‘cluster’ jet) with fine holes or a narrow slit into a coagulation bath with sulphuric acid (H_2SO_4), and salts if spinneret is used. In this step the cellulose xanthate is regenerated back to

cellulose II, while the CS_2 goes into the coagulation liquid, leading to the formation of cellulose filaments. After regeneration the cellulose filaments are washed, an essential step for the removal of contaminants such as H_2SO_4, $ZnSO_4$, Na_2SO_4, H_2S, CS_2 and by-products from spinning reactions. Normally the wash sequence is conducted in six steps; acid wash water, Na_2S/NaOH wash (desulphuhrization), water wash, bleaching (peroxide or NaClO), acid water wash, and finally a second water wash. The final product depends on the chosen extrusion nozzle used during the spinning and is either rayon fibers or cellophane for spinneret and narrow slit respectively. [10] [18] [40]

Shortly before the spinning, additives such as spinning aids, modifiers, and pigments can be added to the viscose dope. Fatty acid or fatty amine ethoxylates are common spinning aids while titanium dioxide (TiO_2) can be added if dull or matt fibers are desired [40]. Zinc sulphate ($ZnSO_4$) may be added as a modifier to create an intermediate, zinc cellulose xanthate, thought to have a greater crystallinity and enable cross-linking between cellulose chains, and therefore initiating a greater orientation of the fibers [40]. Typical tenacity of the obtained filaments is 15–25 cN tex^{-1} with an elongation capacity of 15–27 % [52].

2.4.2 The Lyocell process

Lyocell was developed due to the ambition and desire to improve the performance and cost profile of viscose rayon and came to count as the first new generation cellulosic fibers. Almost 100 years after the patent of viscose, the first commercial samples of lyocell were produced in 1984. The spinning technique used in the lyocell process is dry-jet wet spinning, i.e., a non-derivatizing system [29].

For the lyocell process, a pulp of high quality is required, and the DP is typically in the range of 400 to 1000. The pulp is shredded to obtain small pieces which are mixed at 70 to 90 °C with a 76 to 78 % amine oxide solution (NMMO(aq)) and a small quantity of degradation inhibitor. Additionally, other additives might be added. The result is swollen pulp fibers, also called premix, which inhibit a consistency of dough. The premix is heated (roughly 90 to 120 °C) under vacuum to remove the water, resulting in a clear viscous solution of cellulose with a dark amber-color. The solution normally contains 10 to 18% cellulose. Due to the viscous nature of the solution, it has to be pumped at high pressure (up to 180 bar) to the filtration stage, where the solution is filtrated in two steps to remove the impurities which mainly are introduced via the feedstock. [29]

Spinning of the solution is done by splitting it into sub-streams which are directed to several different spinning positions and supplied to a nozzle via a filter by a metering pump. The solution is extruded through multi-filament spinnerets and spun through (pulled through) an air gap, in which the tows are cooled by a gas flow. Subsequently, the tow goes into a spin bath containing a dilute amine oxide solution, where the cellulose is coagulated. Thereafter, the fiber tows from each spinneret are brought together into one large tow band, which is washed with hot demineralized water, fed countercurrent to the tow, in a series of baths. After washing, the fibers are treated in a number of ways, e.g., bleached (if required), treated with soft finish or antistatic finish, and others to give specific properties. Lastly, the fibers are dried in fiber drum

dryers, crimped, and fed to a radial blade cutter after which the fibers are baled (collected). The typical tenacity of the filaments obtained through the lyocell process is 30–40 cN tex^{-1} and the elongation is 5–10 % [52]. [29]

2.5 Carbon fibers

Carbon fiber (CF) is a carbon rich fibrous material (>90 %C) which is used for lightweight composites and can be utilized for multiple purposes, such as construction, automotive, aircraft, marine applications, and wind energy sectors among others. CF is distinguished by its low density, excellent tensile properties, and high resistance to corrosion [7]. The conversion process of PFs into CFs, see Fig. 8, initially starts with a stabilization step in air (200–300 °C) followed by carbonization in an inert atmosphere (1000–1700 °C). In Addition, a high temperature graphitization step, in an inert environment, can be carried out (2000–3000 °C). [1]

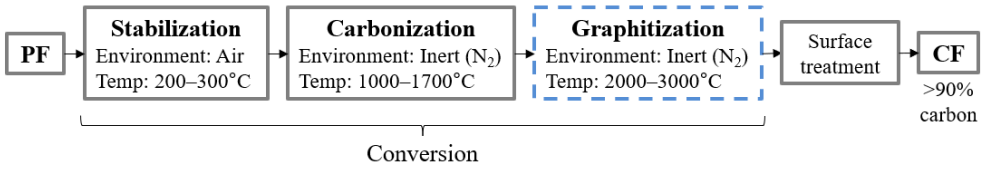

Figure 8. Schematic overview of the conversion process from PF into CF.

The CF market cover a wide range of CF qualities with different mechanical properties that can be tailored to the desired application. Nevertheless, the principal raw material used for CF manufacturing is the petroleum-based polyacrylonitrile (PAN) precursor, which stands for roughly 96 % of the production [1]. Other commercially used precursors for CF production are petroleum-based pitch and Rayon (cellulose-based).

The thermal properties of the PFs are important when it comes to their potential use in CF production. The glass transition temperature, T_g, is for example important as it strongly correlates to its reactivity during stabilization and to the materials melt-ability [7].

PAN-based fibers can be produced through a variety of techniques, such as dry spinning, wet spinning, dry-jet wet spinning, and gel spinning. Additionally, PAN can, even though the polymer by nature degrades before effectively melting, be spun by a highly specialized melt spinning technique [1]. The effect of increasing the final heat treatment temperature of the PAN CFs are an increased tensile modulus, as well as an increased electrical and thermal conductivity [53] [54]. The commercially available PAN-based CFs have an approximate tensile strength (TS) in the range of 3–7 GPa and a tensile modulus (TM) of 200–600 GPa [1] [55].

Petroleum and coal-tar pitch consists of various complex aromatic hydrocarbons. Both petroleum and coal-tar pitch may be extracted and are isotropic by nature and can be used to produce CFs of general purpose grade. However, in order to obtain high performance CFs the isotropic pitch must first undergo a treatment converting the pitch into a mesophase pitch, which leads to a highly liquid crystalline phase with high anisotropy [1]. The pitch-based PFs are obtained by melt spinning which

thereafter undergoes stabilization, carbonization and if desired graphitization, to obtain CFs. The commercial pitch-based CFs usually have a TS in the range of 1.1–3.9 GPa and a TM between 54–965 GPa [1] [55].

Rayon-based PFs are produced through solution spinning, as the cellulosic material will degrade before melting. The commercial Rayon-based CFs generally have a TS around 0.5–1.2 GPa and a TM of up to 100 GPa [56]. However, by applying high temperature graphitization with stretching (>2000 °C), CFs with higher TS and TM can be achieved, such as Thornel 75 CF which has a TS of 2.6 GPa and a TM of 517 GPa [57].

An illustrative summary of the mechanical properties of various commercial CFs obtained from PAN, pitch and Rayon based PFs, is presented in Fig. 9. It is clear that the tensile properties of CFs span a wide range, which makes it possible to highly tailor the mechanical properties of the resultant CF composite towards a specific application.

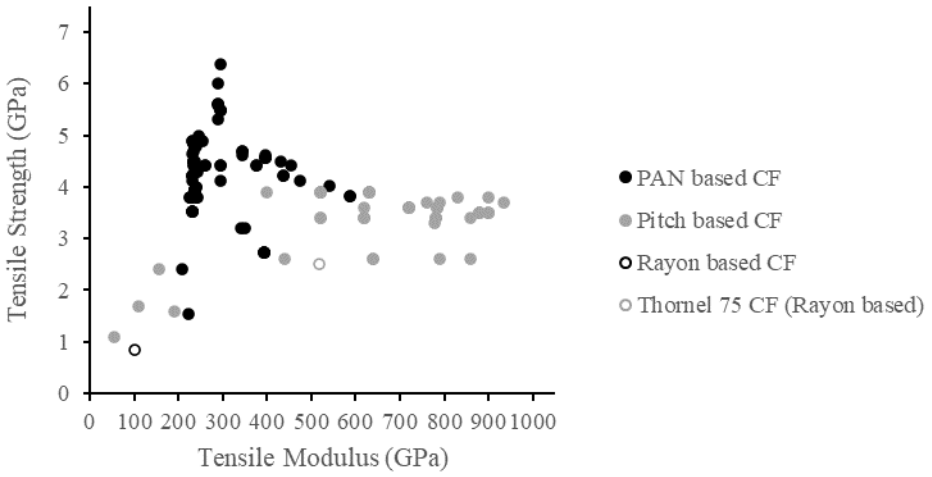

Figure 9. Tensile properties of commercial carbon fibers from PAN, pitch and Rayon [55] [58] [59].

Further development of other CF precursors is ongoing, often with the purpose of either utilizing a renewable precursor and/or lowering the production costs. However, the desired mechanical properties of pure lignin-based CFs (melt spun) has not yet been achieved, and the TM and TS range between 40–85 GPa and 0.39–1.07 GPa, respectively [1] [60] [61]. In addition, the melt spun lignin precursors are brittle and also requires very long stabilization times, hampering its commercial success. In order to solve these challenges, new ways of producing PFs are needed, which is the purpose of this thesis work.

3 Materials and methods

In this chapter the dope preparation, wet spinning procedure and analyses of the study are described.

3.1 Materials

The cellulose source used was a pre-hydrolyzed softwood kraft pulp (SKP, spruce/pine) of dissolving grade. After cooking, the SKP underwent oxygen delignification, followed by ozonation and finally bleaching in two stages with chlorine dioxide, resulting in a SKP with a final intrinsic viscosity of 260 ml g^{-1} with an estimated DP (Mn) of 389. The SKP was obtained from RISE Bioeconomy and health in Stockholm. Further information regarding the SKP can be found in *Brännvall et al.* [62].

Selected lignin for the dope was a softwood kraft lignin (SKL) with a dry solid (DS) content of 58.7 wt.%. The SKL had been produced by the LignoBoost process and was obtained from LignoDemo in Bäckhammar, Sweden. The organic composition of the SKL was 12 mg g^{-1} carbohydrates, 940 mg g^{-1} Klason lignin, and 63 mg g^{-1} acid soluble lignin, while having an elemental composition of 64 wt.% C, 25 wt.% O, 1.4 wt.% S, 5.4 wt.% H, and 0.11 wt.% N. The ash content was below 1 wt.%. Further information regarding SKL can be found in *Bengtsson et al.* [6].

Zinc oxide (ZnO, >99.9 %) was purchased from Alfa Aesar (Kandel, Germany) and sodium hydroxide (NaOH, >99.0 %), analytical grade of sulphuric acid (H_2SO_4, 95–97 %) and sodium sulfate (Na_2SO_4, >99.0 %) were purchased from Merck (Darmstadt, Germany).

3.2 Cellulose-lignin dope preparation

The SKP (10 wt.%) was swelled overnight in water containing 5 wt.% NaOH. Thereafter, a mixture of deionized (D.I.) water, ZnO, and NaOH was added to the system adjusting the concentrations to 5.5 wt.% cellulose, 8 wt.% NaOH, 1.5 wt.% ZnO and water. Dissolution of the cellulose fiber pulp was then achieved after mixing at 60 rpm in a container with baffles cooled by a cooling circulator *Ministat 240* (Huber Kältemaschinenbau AG) utilizing a temperature profile of -10 °C for 8 min, increased to -5 °C for 12 min, and finally at -0.5 °C for 12 min. Successful dissolution was confirmed by observation of the dope in a light microscope, *Axioshop 50* (Zeizz). Filtration of the cellulose dope was done in a Nutsch filter type 3 (Büchi AG) over a 70 µm sintered filter using nitrogen gas. Subsequently, dope deareation was done by centrifugation in a high-speed brushless centrifuge *MPW-350* (MPW Med. Instruments) at 5000 rpm for 15 min.

SKL was added in powder form to the cellulose dope while stirring by hand with a spatula. The quantity of SKP was held constant, at either 4.5 wt.% or 5.5 wt.%, while added SKL varied depending of sought cellulose lignin ratio. An additional filtration step over a 32 µm sintered filter after addition of SKL was carried out for some of the dopes. Deareation of the lignin-containing dopes were done for 3 h while being placed in a cooled beaker at a pressure below 3.5 kPa.

The different dopes are presented as the absolute weight fraction of SKP, C#, dash relative weight fraction of SKL in the dope, L#, i.e., C5.5-L0 for pure 5.5 wt.% SKP dope, C4.5-L30 for a 4.5 wt.% SKP with SKL added in a SKP/SKL ratio of 70/30 wt./wt., and so on. The addition of a dash F indicates that the dope underwent the extra filtration step during dope preparation. The PFs are named after used dope followed by a dash and the number of wash baths, B#, used during the wet spinning.

3.3 Precursor fiber preparation

PFs were produced by wet spinning of the dopes using a bench-scale spinning system, DISSOL, according to the generic scheme presented in Fig. 10. The system consisted of a gear pump, spin head, coagulation bath, washing baths, drying cylinder and a winding bobbin.

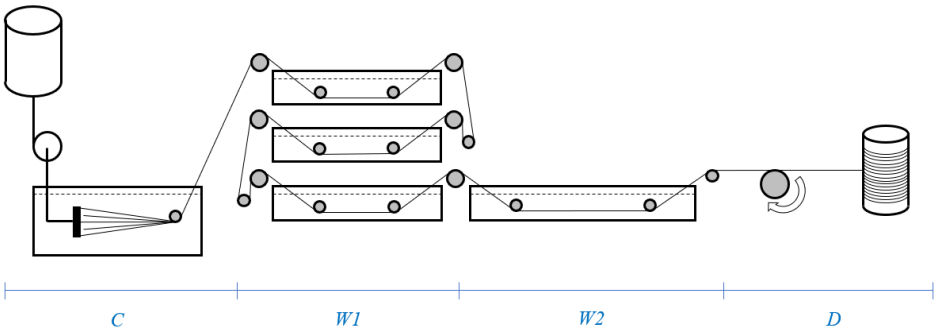

Figure 10. The wet spinning equipment used for the trails can be divided into four sections. Section C includes dope storage and coagulation bath, W1 and W2 are wash and drawing sections, followed by section D containing a drying cylinder and filament collection.

The dope was stored at 4 °C until the start of each spinning trial. A 50 ml syringe, for dope storage, was used allied to a gear pump feeding the dope at a flow rate of 1 ml min^{-1} to a nozzle with a multi-filament spinneret (100 holes, Ø 100 µm), providing an extrusion velocity (m s^{-1}), v_e, according to Eq. 1.

$$\frac{\dot{V}}{A \cdot x_{holes}} = v_e \quad (1)$$

Where $\dot{V}$ is the flow rate in ml s^{-1}, A the area of each spinneret hole in m^2, and x_{holes} the number of spinneret holes. The dopes were extruded into a coagulation bath, 0.25 m, consisting of H_2SO_4 (10 wt.%) and Na_2SO_4 (15 wt.%). The residence time in sec for coagulation, t_{RC}, was found by Eq. 2.

$$t_{RC} = \frac{L_C}{v_r} \quad (2)$$

Where L_C is the length in m of the coagulation bath and v_r is the velocity of the moving roll following the bath in m s^{-1}.

Wash baths in section W1, each 0.38 m, were filled with D.I. water (ambient temp.) and equipped with speed-adjustable rolls for stretching of the filaments. Two different wash bath setups were used, only differing in numbers of baths in section W1, one and three baths respectively. The wash bath in section W2, 0.75 m, contained D.I.

water and 1 wt.% fabric softener *Neutral*® (Unilever) to improve later fiber handling. The residence time in sec for washing, t_{RW}, was found by Eq. 3.

$$t_{RW} = \frac{L_{W1(1)}}{v_{r(1)}} + \frac{L_{W1(2)}}{v_{r(2)}} + \frac{L_{W1(3)}}{v_{r(3)}} + \frac{L_{W2}}{v_{dc}} \quad (3)$$

Where $L_{W1(\#)}$ is the length in m of the baths in section W1, $v_{r(\#)}$ the velocity of the moving roll following each bath used in m s^{-1}, L_{W2} the length, in m, of the bath in section W2 and v_{dc} the velocity of the drying cylinder in m s^{-1}.

The washed filament tow was dried on a drying cylinder (4 laps, Ø 80 mm) at 80 °C followed by subsequent filament collection on a winding bobbin at a velocity, v_{cb}, of 2.8 m min^{-1} respectively 3.1 m min^{-1} when a total of two or four wash baths were used. Total draw ratio, DR_T, of the filament tow was found through Eq. 4.

$$DR_T = \frac{v_e}{v_{cb}} \quad (4)$$

Where extrusion velocity, v_e, and collection bobbin velocity, v_{cb}, both are given in m s^{-1}.

3.4 Preparation of carbon fibers

Prior to stabilization and carbonization, the PFs were fixed on a graphite bridge to prevent fiber shrinkage. Stabilization was performed in presence of air (7 l min^{-1}) in a muffle KSL-1200X furnace (MTI Corporation) at a heating rate of 1 °C min^{-1} from room temperature to 250 ºC at which it was held isothermally for 1 h. The fixed stabilized PFs were subsequently carbonized in a Model ETF 70/18 (Entech) tube furnace equipped with a ceramic (Al_2O_3) tube (70 mm diameter × 1180 mm length). The graphite bridge was placed in the tube furnace, vacuum was applied for 3 × 5 min, and a N_2 flow of 200 ml min^{-1} was applied before starting to heat at 3 °C min^{-1} to 1000 °C. [6]

The gravimetric yield was evaluated by placing 36 ± 4 mg of the PFs in a ceramic crucible, which was placed together with the fixed PFs in the tube furnace during the conversion.

3.5 Characterization

Obtained fibers were evaluated with respect to morphology, linear density, tensile properties, pyrolysis yield and ash content.

3.5.1 Dope stability

The stability of the dopes was examined by observing samples of the C5.5 dope series with SKP/SKL (w/w) ratios 100/0, 90/10, 80/20, 70/30, and 60/40, stored in a fridge at 5 °C for 14 days.

3.5.2 Dope viscosity

The flow rate of the dopes was measured by noting the time it took for 1 ml to be emptied from a 10 ml glass pipette. Subsequently, the kinematic viscosity, $\frac{\mu}{\rho}$ m^2s, was found through Eq. 5.

$$\frac{\mu}{\rho} = \frac{\mu_{ref} \cdot t}{\rho_{ref} \cdot t_{ref}} \quad (5)$$

Where μ_{ref} is the viscosity of water in mPa·s, ρ_{ref} the density of water kg/m^3, and t_{ref} the time for 1 ml of water to pass through the pipette used for measurements. Values for water viscosity and density were obtained from *Mörtstedt et al.* [63].

3.5.3 Fiber morphology

The morphology, i.e., surface and cross section of the PFs, were evaluated in a *Hitachi SU3500 scanning electron microscope* (SEM) (Hitachi) operating at an acceleration voltage of 3 kV with a secondary electron (SE) detector. The PFs were positioned on a sample holder using double-sided carbon tape, and the cross-sections were prepared by snapping the fibers in liquid nitrogen. Prior to the analysis the PFs were Ag-coated by a *108 auto sputter coater* (Cressington Scientific Instruments Ltd.).

3.5.4 Pyrolysis yield

The thermal degradation of the raw materials and PFs was analyzed by thermogravimetric analysis (TGA) in a *TA Instruments Q5000 IR*. Sample size used for analysis was 10 ± 1 mg and 3.5 ± 0.5 mg for raw materials and PFs, respectively. The samples were heated at 10 °C min^{-1} to 1000 °C in nitrogen (25 mL min^{-1}). The pyrolysis yield was determined as the residual mass at 1000 °C after being normalized to its dry content.

3.5.5 Tensile properties

Single fiber tensile tests were performed on conditioned PFs (20 ± 2 °C and 30 ± 3% relative humidity (RH)) on a *LEX820/LDS0200 fiber dimensional system* (Dia-Stron Ltd.). A fixed gauge length of 20 mm and an extension rate of 5 mm min^{-1} were employed during testing. The fiber diameter was determined by a reflected light illumination microscope *Olympus BX51M* (Olympus Corp.), while the linear density (dTex, g/10,000 m), ρ_l, was obtained through Eq. 6.

$$\rho_l = \frac{10{,}000 \cdot m_{fiber}}{n \cdot L_{fiber}} \quad (6)$$

Where m_{fiber} is mass in g of fiber tow, n the number of fibers in the tow, and L_{fiber} the length of the fiber tow in m. Evaluation of the results was completed with the *UvWin 3.35.000 software* (Dia-stron Ltd.), and the reported values are the average of 30 to 35 individual single filament tensile tests.

3.5.6 Ash content

The ash content was determined in air at 525°C according to *ISO 1762* in a *TA Instruments Q5000 IR* [64].

3.5.7 Ash composition

The elemental composition (wt.%) of the ash (from TGA) was estimated by *energy dispersive X-ray analysis (EDXA)* (XFlash detector, Bruker Corp.) using a back scattering electron (BSE) detector at a 10 mm working distance with an acceleration voltage of 10 kV. Elements of specific interest were Na, S, and Zn. Obtained data was evaluated with the *Esprit v.1.9.3. software* (Bruker Corp.).

4 Results and discussion

The experimental part of this thesis work started off with the preparation of a variety of dopes which were evaluated with respect to their stability and appearance prior to being utilized for wet spinning of PFs. After several successful spinning trials two of the produced PF samples were chosen and converted into CF, whereafter all fibers (PFs and CFs) were evaluated.

4.1 Dope preparation and stability

Two series of SKP dopes, with absolute concentrations of 4.5 wt.% and 5.5 wt.%, were successfully produced. From these two SKP dopes through the addition and dissolution of SKL two dope series were obtained, one with the absolute cellulose concentration of 4.5 wt.% with three different SKP/SKL ratios (100/0, 70/30, and 65/35 wt./wt.), and a second with the absolute cellulose concentration of 5.5 wt.% with five different SKP/SKL ratios (100/0, 90/10, 80/20, 70/30, and 60/40 wt./wt.). Hence, providing a total of eight unique dopes with SKP/SKL ratios between 100/0 and 60/40 (wt./wt.), see Tab. 8 in App. 1. The total dope concentrations ranged from 4.5 wt.% to 9.2 wt.%.

The obtained dopes of SKP-SKL blends had a dark color which made it difficult to visually determine if a complete and even dissolution of SKL had been achieved. However, when adding the additional filtration step with a 32 µm sintered filter no solid lumps of SKL could be observed, indicating a full dissolution of the added lignin in the dopes up to the highest concentration, 9.2 wt.%, evaluated. Moreover, the dopes appeared homogenous, with no darker or lighter parts being observed during stirring or pouring, indicating that an even distribution of the SKL was achieved.

The viscosity of the dope is a highly important parameter for solution spinning (both for wet and dry-jet wet spinning). Due to the dark color and the limited amount of dope the number of suitable methods for viscosity measurements became restricted. The method which came to be used has a high uncertainty margin which was estimated to be approximately ±10%. Nevertheless, the measurements gave an estimation of how the dope concentrations and the SKP/SKL ratios affected the viscosity.

Depicted in Fig. 11 is the kinematic viscosity of all prepared and spun dopes with an additional baseline with solutions of 8.0 wt.% NaOH, 1.5 wt.% ZnO and SKL ranging from 0.0 to 3.7 wt.%. The 4.5 wt.% dopes had a viscosity of 1.2×10^{-4}–1.6×10^{-4} m^2s while the 5.5 wt.% dopes were in the range of 3.8×10^{-4}–7.8×10^{-4} m^2s, suggesting that the viscosity was mainly affected by the SKP concentration. This observation was supported by the baseline viscosity of 1.1×10^{-6} m^2s, which was constant for the investigated range of SKL concentrations. It is worth to note that the maximum SKL concentration (3.7 wt.%) corresponds to the highest concentration used in the dopes for fiber spinning. The fact that the SKP has a greater effect on viscosity than the SKL is not surprising, since the SKP has a much higher molecular mass and is a linear polymer. However, the dope viscosity does not seem to be affected by the SKP-SKL ratio, with the exception of the C5.5-L40 dope (total dope conc. 9.2 wt.%) which

seemingly has a viscosity almost twice as high as the other four C5.5 dopes in the series. Therefore, it may be assumed to be a breakpoint where either the total dope concentration and/or the SKP-SKL ratio and the interaction between SKP and SKL will come to affect the viscosity.

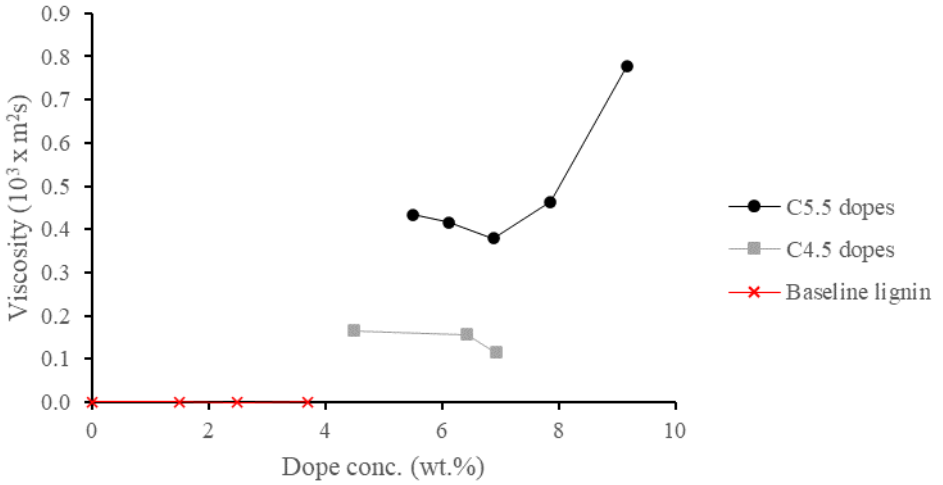

Figure 11. Kinematic viscosity of spinning dopes, 5.5 wt.% SKP series and 4.5 wt.% SKP series, and baseline (only dope solvent and added SKL).

Regarding the deaeration of the dopes it was noticed that an increasing dope viscosity seemed to aggravate the process. Additionally, the low temperature (~5 °C) at which the dopes were held during deaeration might have been a contributory factor to impede the deaeration, as oxygen/air is more soluble at low temperatures (Henry's law), which has been mentioned as a possible reason by *Vehviläinen* [65]. *Vehviläinen* suggests that a temperature equal or higher than the wet spinning temperature should be used during deaeration. However, this issue needs further investigation to be fully ruled out and is not the prime focus of this work. In addition, other factors such as the presence of particles and salts, as well as the decreased pressure used during deaeration, will also affect the air/oxygen solubility within the dope and should thereof be taken into account.

The stability of the dopes was examined by a very simple method but made it possible to estimate the stability time while giving some insights. The purpose of adding ZnO to the dope is to improve solubility and increase the time until gelation starts, whereas gelation will start within 2 days (depending on storage temperature) without a stabilization agent such as ZnO [66]. The aim was to evaluate whether the addition of SKL and an increased SKP/SKL ratio had any impact on dope stability, i.e., time to gelation. From the stability tests it was observed that an increasing dope concentration and/or SKL ratio reduces the stability time, see Tab. 4. However, it is difficult to set a time limit for when the gelation starts, but all investigated dopes appeared to be stable for the time period passing between manufacturing until being spun (<three days). Nevertheless, dope stability is an important factor for further development of

the process and should therefore be more thoroughly investigated, e.g., by rheology measurements as opacity makes optical methods unsuitable.

Table 4. Stability observation of C5.5 dope series stored in fridge at 5°C.

Sample	Week 1	Week 2
C5.5-L0	No visible change.	Small shift in appearance at the end of the week.
C5.5-L10	No visible change.	Small shift in appearance at the end of the week.
C5.5-L20	No visible change.	Small shift in appearance at the end of the week.
C5.5-L30	No visible change, small shift in appearance at day 5.	Possible start of gelling day 12, Flowed partially when beaker was tipped.
C5.5-L40	No visible change, small shift in appearance at day 4, possible start of gelling day 6.	Did not flow when beaker was tipped on day 12, but after gentle stirring flowed when beaker was tipped.

4.2 Precursor fibers

In this section results regarding wet spinning trials and evaluation of the PFs will be presented.

4.2.1 Wet spinning trials

All the prepared dopes were spinnable and continuously spun for a few minutes up to approximately 15 minutes. However, PFs were not successfully spun from the C5.5-L40 dope until an additional 32 µm filtration and deaeration step was conducted. The color of obtained PFs gradually darkened with increased SKL content, as depicted in Fig. 12, which suggests that the process is able to produce PFs without major leaching of SKL into the coagulation and wash baths. Furthermore, the coagulation and wash liquids did not change color and no precipitated SKL was found in the baths. Together, this indicates no or small SKL losses during spinning in the used system setup.

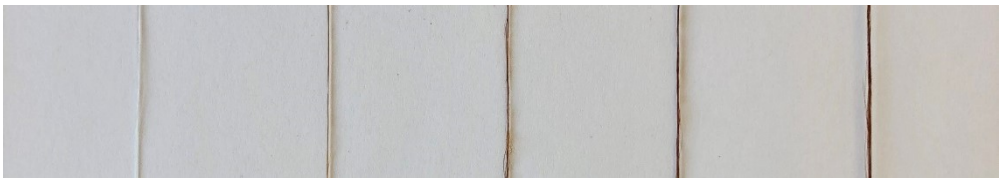

Figure 12. Seen from the left: PFs obtained from 5.5 wt.% SKP dopes with SKP/SKL ratios (wt./wt.) of 100/0, 90/10, 80/20, 70/30, and 60/40.

The variations in viscosity and SKP/SKL ratio seemed to have little or no effect on the spinnability. Problems regarding the spinning seemed to be more affected by air

bubbles remaining in the dope, leading to clogging of the spinneret and fiber breakage. However, this is likely an indirect effect of the dope viscosity, as an increasing viscosity make deaeration of the more viscous dopes more difficult. Additionally, observations were made indicating that air which had remained in the pump casing gradually was pulled along with the dope during the initial extrusion (creating new bubbles within the dope). From an experimental setup point of view, the speed-adjustable rolls in section W1 (Fig. 10) also created problems as the fiber tow in some cases began to wind up on the rolls which resulted in fiber breakage. Both deaeration and winding problems can most likely be tackled by minor adjustments in the experimental setup. However, optimization of the spinning parameters was not included within the aim of this thesis work and was therefore not approached at this time.

The theoretical draw ratio of the PFs were 2.2 and 2.4 when using two and four wash baths, respectively. However, during spinning the draw ratios came to vary between the different spinning trials, and the actual draw ratios can be found in Tab. 10 in App. 2. The reason for this is a change in the relative speed of the fiber tow in the spinning line as a result of spinneret clogging and that some individual filaments break. Spinneret clogging leads to a decreased extrusion area while the flow rate of the dope out from the pump is kept constant, resulting in an increased extrusion velocity. Therefore, in combination with a constant fiber up-take speed at the end of the spinning line, the draw ratio will decrease.

As it might be assumed, the linear density of the PFs obtained from the different spinning trials were affected by the actual draw ratio, as illustrated in Fig. 13, and as expected a decreasing draw ratio result in an increasing linear density. The variations in linear density were found to be high and in the range of 2.0–9.6 dTex, with measured fiber diameters in the range of 15–32 µm.

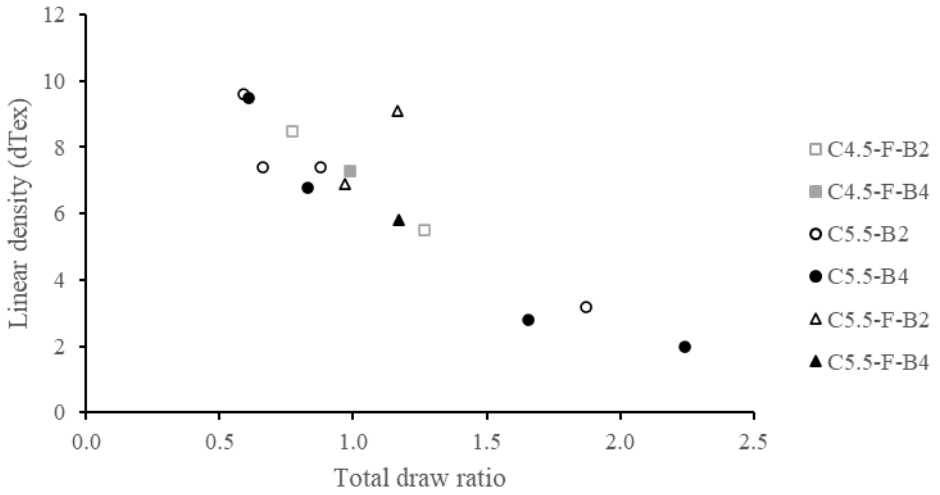

Figure 13. Correlation between total draw ratio and linear density of PFs (B2 = two baths and B4 = four baths).

4.2.2 Morphology of precursor fibers

The fiber morphology is an important characteristic of a PF as it may affect the tensile properties of the PF and the resultant CF. Therefore, the fiber morphology of the spun PFs using different SKL/SKP ratios and total dope concentrations was evaluated with SEM (Fig. 14a–d). Irrespective of amount of SKL and dope concentration, no significant difference in morphology could be observed. The PFs display striations parallel to the longitudinal direction of the fibers, in line with the morphology usually observed for wet spun viscose fibers [67]. Notably, the morphology of the PFs in the present work is more similar to viscose fibers than the one of air gap spun lyocell fibers, as the latter usually has a more circular cross section and smoother surface. This is likely related to the high similarity between the coagulation conditions in the viscose spinning system and the cold NaOH(aq) solvent system used in the present work. Both these systems use NaOH-water as the solvent, and the coagulation bath used in this work (H_2SO_4/Na_2SO_4) is actually the one used in the viscose process. This suggests that further development of this solvent system adopt knowledge from the viscose process to alter e.g., fiber morphology. Furthermore, the PFs had a solid cross-section with no visible pores. However, variations in fiber shape could be observed, going from circular/oval into a kidney-shape, as can be seen in Fig. 14(a), and in some cases flattened.

The initial diameter of the PFs may be the reason for the variation in cross-sectional shape, as the thickness of the fiber will affect the diffusion distance for the dope solvent. An additional affect of the variation in thickness of the PFs is that it might influence the efficiency of the drying step. Hence, resulting in e.g., flattened fibers, which might be a result of fibers still containing moisture when collected on the bobbin and thereafter having a decrease in moisture content while in a fixed position.

As a result of the strained surface and non-circular shape of the cross sections, textile measures (cN/Tex) should be used instead of diameter (cross sectional area) when evaluating the tensile properties. The linear density, in dTex, for each PF sample is presented in App. 2 Tab. 10.

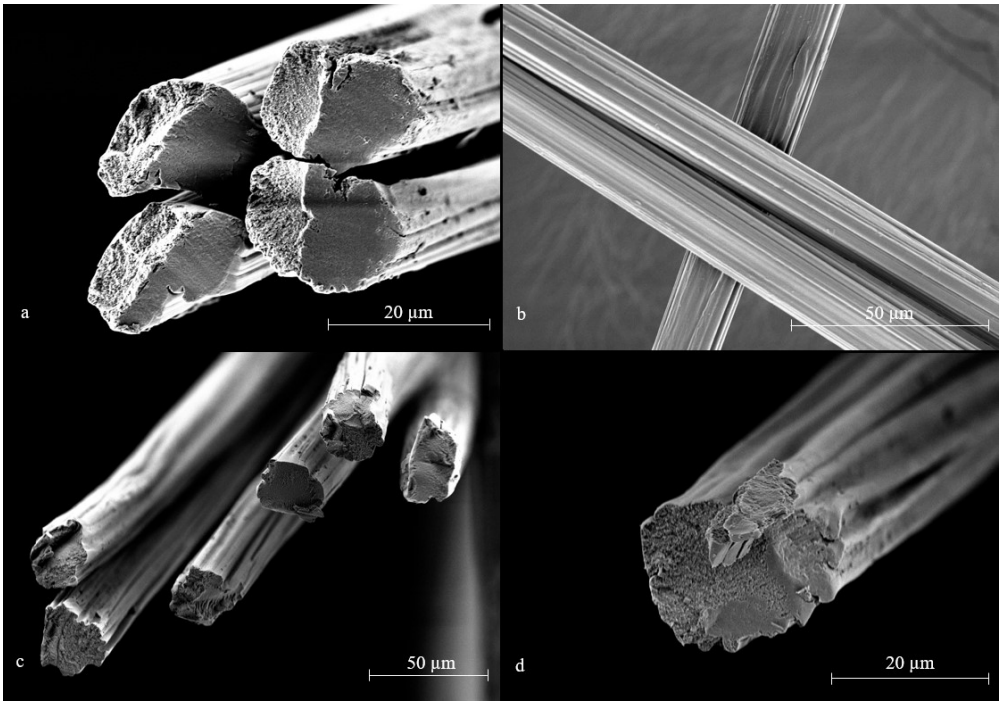

Figure 14. SEM images of PFs (a) cross-section 5.5 wt.% SKP with SKP/SKL 100/0 wt./wt., (b) surface 5.5 wt.% SKP with SKP/SKL 90/10 wt./wt., (c) cross-section 5.5 wt.% SKP with SKP/SKL 70/30 wt./wt., and (d) cross-section 4.5 wt.% SKP with SKP/SKL 65/35 wt./wt..

4.2.3 Ash content of precursor fibers

The ash content of the PFs were evaluated due to the desire and requirement of keeping the ash level as low as possible when producing CF for structural applications. It is known that high levels of inorganics (ash) may contribute to the development of a porous structure of the resultant CF, which usually results in a decrease in the mechanical properties as the risk of defects increases. A guideline could be to keep or strive for an ash content of <1 wt.% [61].

Theoretically, the total residence time when using two or four wash baths were 25 and 39 seconds, respectively, thus leading to a roughly twice as long residence time when four baths were used. From the ash content analysis, it is clear that the increased wash residence time had a positive effect on reducing the ash content of the spun PFs, see Fig. 15. The ash content was lower for all PFs that had passed four baths, compared to their counterpart which had only passed two.

The ash contents of the PFs (0.6–23.9 wt.%) were relatively high compared to the raw materials (SKP 0.1 wt.%, SKL 0.6 wt.%). This suggests that salt from the dope and the coagulation bath were present in the PFs, even after the washing sequence.

Irrespective of the number of wash baths, it was noted that the wash of the C5.5 PFs appeared to be more efficient than of the C4.5 PFs, as the latter had a notably higher ash content both when using two and four baths, see App. 3 Tab. 11. However, it should be noted that both series were spun using the same settings which might have been more suitable for the more viscous series C5.5. For example, the lower content of solids in the C4.5 series leads to a larger portion of dope solvent that must be

withdrawn during coagulation, subsequently there is a possible need of a longer coagulation time than used during these trials. Additionally, with an increasing linear density (diameter) the washing becomes more difficult, as the diffusion length for the solvent out of the fiber becomes longer, which might lead to a higher ash content.

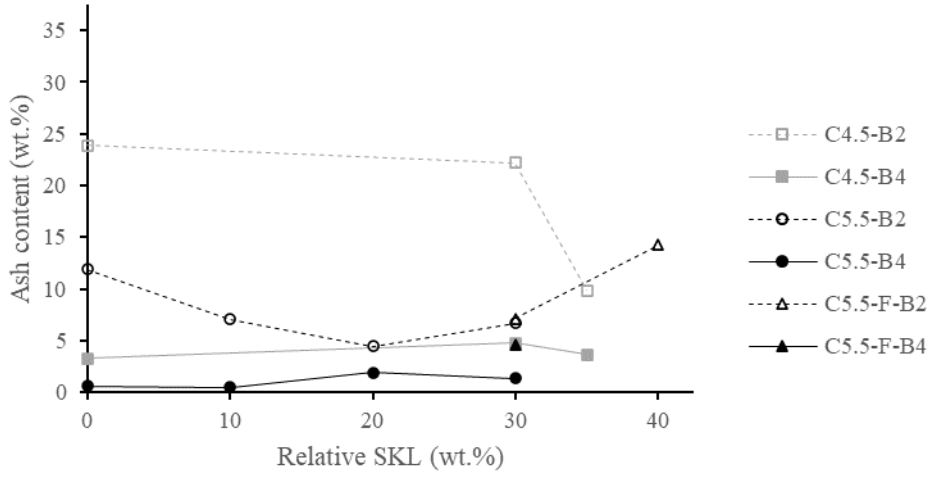

Figure 15. Effect of the number of wash baths and SKP/SKL ratio on the ash content of the PFs. Dashed lines two wash baths, solid lines four wash baths.

Due to the high ash content of the fibers the elemental composition of the ashes was examined with EDX to rule out the origin of added ash components. The EDX analysis of the ashes revealed high levels of Na and S, as well as some Zn, as illustrated in Fig. 16 (see App. 3 Tab. 11 for data). The high content of Na in the ash is expected since it is present in both the spinning dope (NaOH) and the coagulation bath ($NaSO_4$). The S originates from the sulfate in the coagulation bath (Na_2SO_4 and H_2SO_4) and to some extent from the SKL, whereas the residual Zn comes from the ZnO added to the dopes.

Nevertheless, smaller amounts of some other components (K, Ca, and Cr) were also detected. Both K and Ca occurs naturally in wood as nutrients [68]. However, the peak energy for Cr (0.573 keV) is close to the one of O (0.525 keV) and the result lines might be misidentified lines, meanwhile, the peak energy of Na (1.014 keV) is close to Zn (1.012 keV) which also might lead to misidentified lines and a misleading result [69] [70] [71].

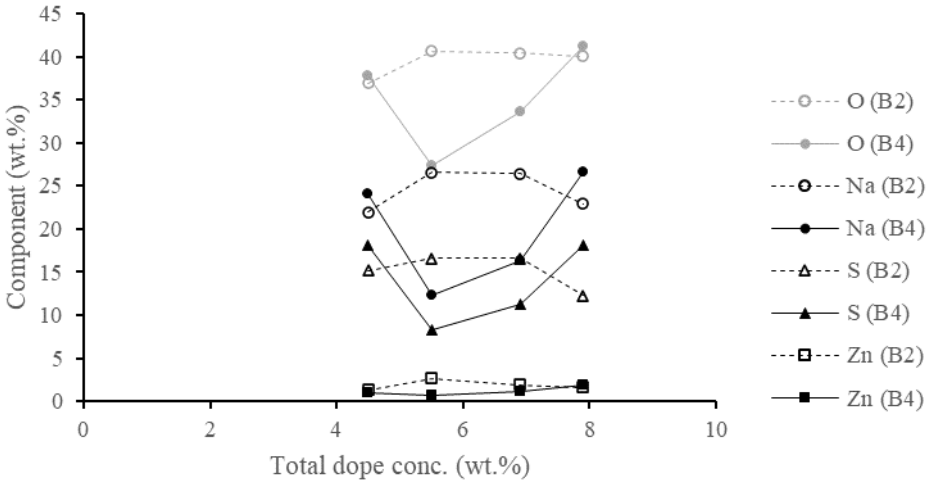

Figure 16. Ash composition of PFs, dashed lines two wash baths, solid lines four wash baths.

4.2.4 Tensile properties of precursor fibers

When evaluating the PFs tensile properties (see summary in Tab. 12 App. 4) with respect to SKP/SKL ratio, both TS and TM seem to decrease with increasing SKL content, see Fig. 17, which was expected. However, there is an exception with L0 and L10 of the C5.5-B2 PFs which might be explained by the high ash content of the C5.5-L0-B2 fiber (11.9 wt.%). The obtained values of TS ranged from 6.4 to 27 cN/Tex, while TM was within the range of 407 to 1450 cN/Tex, which is weaker than viscose fibers but stronger than meltspun lignin fibers. However, it should be mentioned that the fiber tensile properties within this study were measured at around 30% RH while the values in literature often are given for a 65% RH. Additionally, there seems to be a correlation between both TM and TS with the total dope concentration, as both seem to decrease with an increasing total dope concentration use for the production of the PFs (see Fig. 22 App 4).

Moreover, the additional filtration (32 µm filter) of the C5.5-L30 dope had no notable effect on the TS or TM of the obtained PFs. However, it could be argued that the ash content (see section 4.2.3) might have had an effect on the TS and TM, e.g., by creating weak points in the PFs. This, however, needs further investigation in order to be fully ruled out.

Unfortunately, the PFs obtained from C4.5-L0 and C4.5-L30 could not be separated for testing of linear density and tensile properties, probably due to insufficient drying prior to collection on the winding bobbin.

A decreasing linear density gave increasing tensile properties, TS and TM, see Fig. 23 App. 4, and can be explained by Weibull's weakest link principle, meaning that a large volume (thicker fiber) results in a greater probability of a weak point defect [4]. However, three samples deviated from the trend, which may be explained by their lower draw ratio during the spinning. A lower draw in the spinning may inhibit

molecular orientation of the cellulose chains in the preferred longitudinal direction of the fiber, which in turn may affect the TS and TM [8] [72].

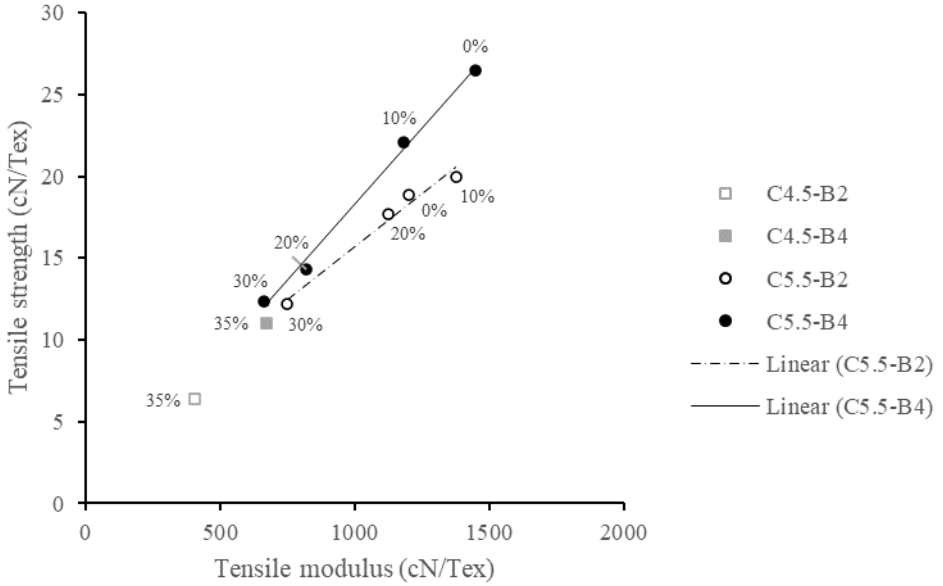

Figure 17. Mechanical properties of PFs, stated %-value refer to the relative SKL concentration.

Fig. 18 shows the strain at break for the PFs, which seem to have a decreasing trend with increasing SKL content for the C5.5-B2 and C5.5-F-B2 series, while increasing for the C5.5-B4 series. All PFs had a strain at break ranging from 1.7 % to 6.6 %. Nevertheless, when adding the standard deviation there is no clear separation among the series until the SKL content increases above 20 wt.%.

However, regarding the effect of the additional filtration step it is noticeable that the C5.5-L30-F-B4 received a lower strain at break compared to C5.5-L30-B4, while no differences were seen between C5.5-L30-B2 and C5.5-L30-F-B2. It may suggest that the comparative results on the strain at break for the PFs, with and without the extra filtration step, instead might be related to the ash content of the PFs (see Fig. 24 App. 4). Subsequently, showing that an extra filtration step did not per se affect the strain at break. To sum up, it could be argued that factors such as morphology, draw ratio, linear density, and ash content all might affect the strain at break. However, this needs further investigations.

A possible factor that might have affected the results of the tensile properties is the uncertainty brought by the human counting of the fibers in the tow for the linear density value, together with the shape of the fibers with a non-circular cross section, which may have led to deceptive values.

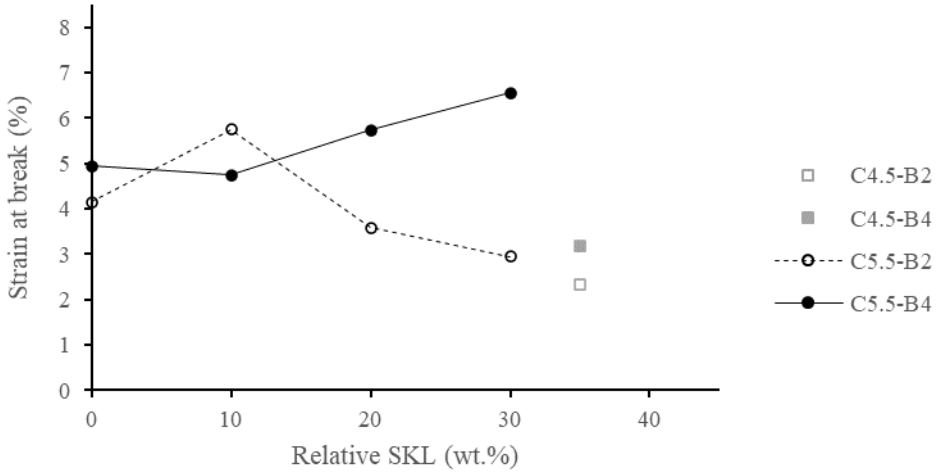

Figure 18. PFs strain property derived via different numbers of wash baths and SKP/SKL ratios. See App. 4 Tab. 12 for details.

4.2.5 Pyrolysis yield of precursor fibers

The yield upon pyrolysis (carbonization) of a PF is an important parameter affecting the final cost of a CF. The purpose of incorporating SKL together with SKP in a PF is to increase the yield after conversion into CF. Therefore, the PFs were pyrolyzed in the TGA to assess the effect of the SKL addition (Fig.19). The pyrolysis yield increased for the PFs that contained SKL, compared to the pure SKP PFs. This was expected as the SKL provides a higher carbon content as well as an aromatic backbone in contrast to the SKP. The residual mass at 1000 °C ranged from 5.3 wt.% (C5.5-L0-B4) to 26.6 wt.% (C4.5-L35-B2) for the PFs when using a TGA for the analysis. A summary of the pyrolysis yield for all samples can be found in Tab. 13 in App. 5.

The mass loss between 25–150 °C in the pyrolysis curves corresponds to the release of moisture from the samples. The neat SKP sample (C5.5-L0-B4) shows a large mass loss between 240–400 °C and a sharp loss around 350 °C typical for the thermal degradation of the cellulose. The sharp mass loss is mainly due to the formation of tar (of which levoglucosan is a major part) and volatiles during the depolymerization [73]. However, a continuously slow mass loss is also observed above 400 °C. [4]

For the PFs with lower ash content (4 baths), the decomposition of the SKL containing PF started at lower temperatures than for the neat SKP PF and had a slightly slower mass loss that occurred over a wider temperature range (200–500 °C). Both range and shape of the weight loss curves shows signs on the presence of the SKL and SKP, as they have obtained some of the typical features found in SKL and SKP pyrolysis mass loss curves [7] [74].

The onset of the major thermal decomposition for the less washed samples (2 baths) started at a lower temperature (~260 °C instead of ~280 °C) than for the more washed PFs and had a lower mass loss that occurred in a wider temperature range (Fig.19), which may be due to their higher content of inorganic salts. For the less washed PFs, a distinct mass loss was also observed at about 700 °C, which could be an indication

on a carbothermic reduction reaction taking place, which has been reported to occur when Na_2SO_4 and carbon co-exists at high temperatures [75]. However, the bump on the curves at this position might also be the residual salt $ZnSO_4$, which has a decomposition temperature of 680 °C [76], still present in the fibers. Hence, it is suggested that optimization of the spinning process, e.g., by adjusting coagulation rate and/or streamline of the washing section, will enable to decrease the ash content (which was found to be as high as 24 wt.% and never less than 4.5 wt.%) of the PFs to a more acceptable level where the thermal decomposition is no longer significantly affected.

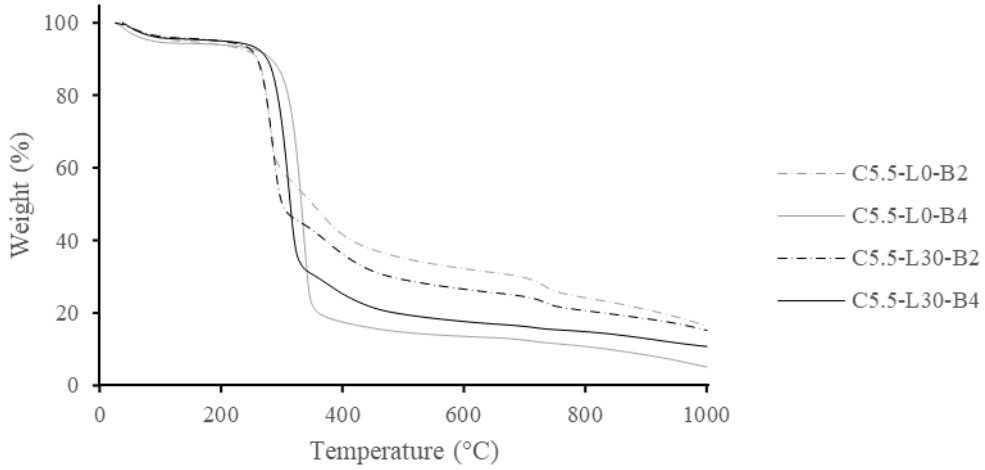

Figure 19. Pyrolysis curves of 5.5 wt.% PFs with no or 30 wt.% relative SKL content at a heating rate of 10°C min^{-1} in nitrogen.

An overview of the pyrolysis yield relative to the theoretical carbon yield for the PFs in correlation to the relative SKL content can be seen in Fig. 20. There is a pronounced difference in yield depending on the wash residence time used, demonstrating the significant contribution from the residual inorganic salts on the yield. Therefore, it can be suggested that the ash content (see App. 3 Tab. 11) has an impact on the obtained yields, as the yield is considerably higher for the less washed PF than its corresponding further washed PF. How and why the salts have an impact on the pyrolysis could be further investigated, do they work as catalysts or/and do they have any other impact? For example, the cation Potassium is known to affect both cellulose and lignin during the pyrolysis.

However, for the C5.5 series (4 baths) it is implicated that an increased SKL ratio will lead to an increased residual mass of the PF when converted to CF. Both the LightFiber project [6] [5] and *Hummel et al.* (e.g., [77] [78]) have shown on similar results. Nevertheless, due to the lack of other publications using the same dope composition and solvent system it is hard to compare results and make further correlations of the impact of adding SKL and its ratios. Therefore, further work and evaluation of this type of PFs are needed to strengthen the assumptions made within this work.

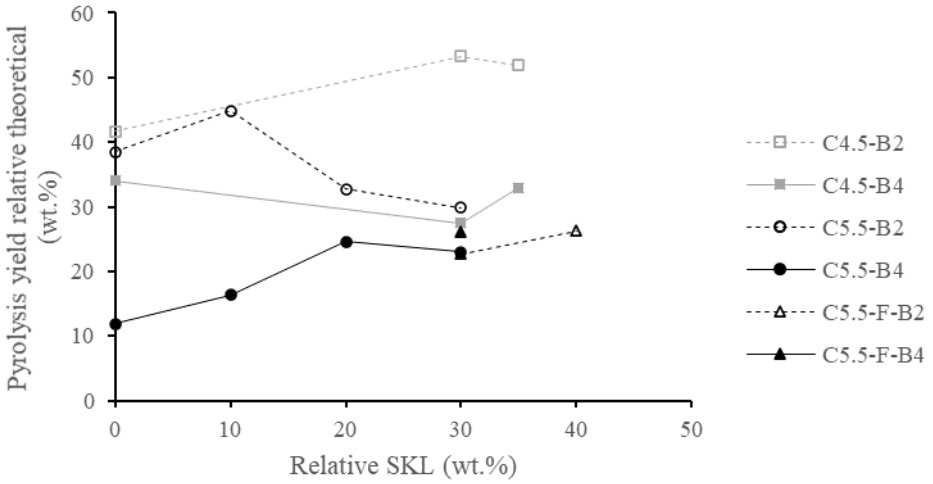

Figure 20. Effect of dope concentration, SKP/SKL ratio and wash residence time on PF pyrolysis yield relative the theoretical.

4.3 Conversion to carbon fiber

The PFs C5.5-L0-B4 and C5.5-L30-B4 were chosen for batch-wise conversion into CFs, which turned out successfully with two different CF batches. Prior to conversion, the PFs were fixed on a custom-made graphite bridge to prevent fiber shrinkage during the thermal treatments, which is known to increase the tensile properties of the CF [74]. The PFs were then successfully converted into CF via oxidative stabilization (250 °C) and carbonization (1000 °C). To the best knowledge of the author, this is the first work reporting CF preparation from wet spun lignin-cellulose PFs using the cold NaOH(aq) solvent system. As the CF manufacturing process is an energy intensive and costly process it becomes of high interest to maximize the conversion yield. The gravimetric conversion yield obtained for C5.5-L0-B4 and C5.5-L30-B4 were 12 wt.% and 28 wt.%, respectively, which indicates that the addition of SKL has a positive effect on the yield. The yields reported in this work are close to the lower and higher limit of the typical cellulose CF yield which is 10–30 % [3].

In this case, when using the method with the ovens to obtain the gravimetric yield of the PFs the yields were higher compared to the results from the TGA measurements, see Tab. 5. However, this is not surprising as the oxidative stabilization step, which is excluded in the TGA measurements, has been shown by *Bengtsson et al. (2018)* to increase the gravimetric yield [6]. The result of the pyrolysis yield with this method was considerably higher with 28 wt.% compared with 11.6 wt.% for the C5.5-L30-B4, which partly may be due to the PFs undergoing the separate stabilization and carbonization steps. Hence, during the stabilization several important reactions occur, e.g., dehydration which stabilizes the cellulose. If a complete dehydration is achieved, it will minimize the formation of levoglucosan and other volatile fragments which causes major mass losses and thereby decreases the conversion yield [4] [79]. An effect when introducing oxygen during stabilization is also the change in the SKL structure (cross-linkage), which as a result makes the SKL more resistant to thermal degradation [80].

Table 5. Gravimetric yield obtained from conversion of the PFs to CFs, during actual conversion (a), and from TGA (b).

Sample	Stabilization yield (wt.%)	Carbonization yield (wt.%)	Total gravimetric yield[a] (wt.%)	Pyrolysis yield[b] (wt.%)
C5.5-L0-B4	98	12	12	5.3
C5.5-L30-B4	94	30	28	11.6

Additionally, the relative gravimetric yield (actual/theoretical) was higher for the CFs made from PFs made from a 30 wt.% SKL (56 %), compared to 0 wt.% SKL (27 %) dope. A reason for this might be that the SKL has a positive impact on the SKP, e.g., by acting as flame retardant protecting the SKP during the conversion [6]. These results suggest that it is possible to increase the gravimetric yield by preparing CFs from a blend of SKP and SKL. This is in agreement with the observations of *Bengtsson et al.* [6]. Nevertheless, there is still room and possibility for further optimization and evaluation regarding the effect of adding SKL to PFs.

The results of the EDXA, see Tab. 6, showed on a CF elemental composition with no remaining Zn. The carbon (C) content of the CFs was similar, 85 and 87 wt.%, when made from neat SKP PFs and when containing 30 wt.% SKL, respectively. The carbon (C) content of the CFs prepared in the present work is lower, compared to the 94 wt.% reported by *Bengtsson et al.* [81]. However, this is not surprising as Bengtsson et al. had CF made from dopes with even higher lignin content (70 % lignin and 30 % cellulose).

The CFs had a rather high oxygen (O) content, see Tab. 6. A way to reduce the content of O is to increase the temperature during the carbonization to allow a continuous elimination of it, or decrease the heating rate and thereby increase the dwelling time. However, in this thesis work a temperature profile more suitable for lignin conversion, while e.g., a higher temperature would be used for the conversion of cellulose. The Sulphur (S), on the other hand, is probably residue left from the coagulation bath or might originate from the SKL.

Table 6. Elemental composition of CFs.

Sample	C (wt.%)	O (wt.%)	S (wt.%)	Zn (wt.%)
C5.5-L0-B4	85	14	0	n.d
C5.5-L30-B4	87	12	1	n.d

The SEM morphology evaluation showed a C5.5-L0-B4 with some longitudinal striation pattern, Fig. 21(a), and a dog-bone shaped cross-section, see Fig. 21(b), while the C5.5-L30-F-B4 CF had a similar appearance to its PF with a longitudinal striation pattern, Fig. 21(c), and a circular-striated cross-section, depicted in Fig. 21(d). These results suggest that the morphology of the PFs is to a large extent preserved into the CF.

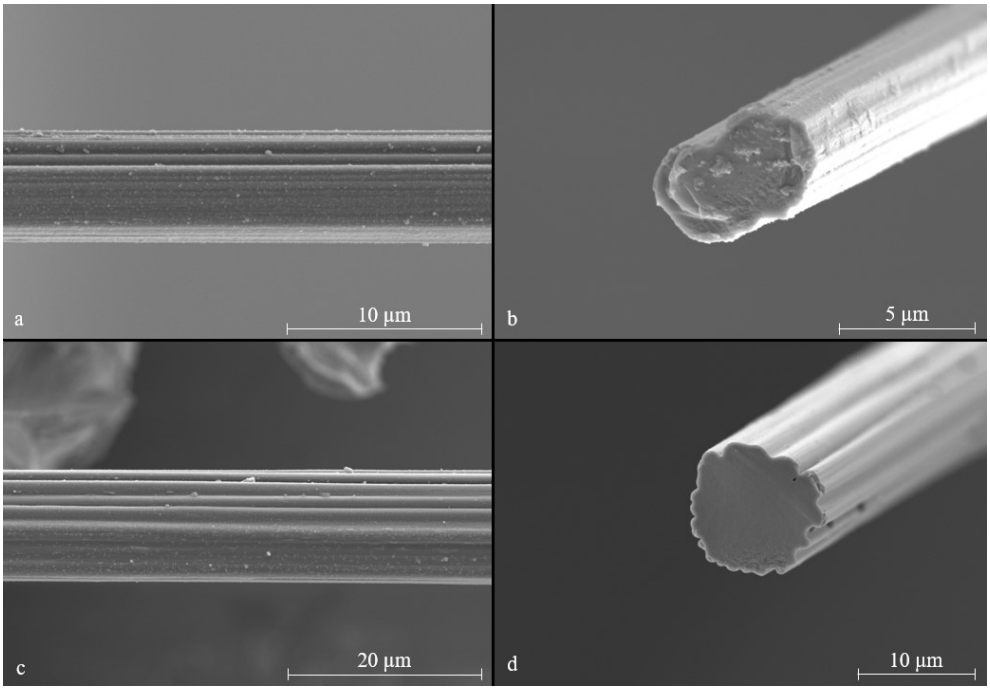

Figure 21. SEM morphology images of CFs, (a–b) SKP-SKL ratio 100/0 wt./wt., and (c–d) SKP-SKL ratio 70/30 wt./wt..

TM and TS increased after conversion of the PFs into CFs for both the neat SKP and the 30 wt.% SKL sample (Tab. 7). The increase of the TM and TS was somewhat higher for the C5.5-L30-B4 CFs, 5.5 and 4.3 times higher respectively, compared to 4.4 and 3.9 times for C5.5-L0-B4. Nevertheless, it is important to note the large difference in diameter of the two CFs obtained. For example, the diameter of a CF is expected to have a certain effect on the mechanical properties as the possibility of critical defects decrease per unit volume of the fiber with a decreasing CF diameter [1]. However, the obtained values of TM and TS for the CFs in Tab. 7 are very low compared to the commercial CFs presented previously in Fig. 9.

Table 7. Tensile properties of CFs.

Sample	Diameter (µm)	TM (GPa)	TS (GPa)	Strain at break (%)
C5.5-L0-B4	6.0 (0.8)	71 (15)	1.17 (0.29)	1.70 (0.30)
C5.5-L30-B4	13.1 (0.8)	51 (6)	0.67 (0.12)	1.31 (0.19)

Bengtsson et al. have investigated the effect of stabilization conditions and diameter on the mechanical properties [74]. The CFs in the study by Bengtsson were obtained from cellulose-SKL 30/70 (wt./wt.) blends, and both the thin CF (6–8 µm) and thick CF (13–15 µm) had similar TS as the SKP/SKL blend CF produced within this thesis work. However, compared to the TM obtained in this work (51 GPa), Bengtsson and co-workers reported a slightly higher TM for the thin (76–77 GPa) and thick (64–66 GPa) CFs. Possible reasons for the lower TM are hard to determine, however,

Bengtsson et al. had much more lignin in their fibers, a higher D.P. cellulose, and a lower ash content. Nevertheless, it might also be due to the operating conditions which could be further adjusted and tuned for the specific system used.

The strain at break of the fibers had decreased for both samples, which was expected.

5 Conclusions

This thesis work reports the preparation of CFs from SKP-SKL PFs wet spun from with the cold NaOH(aq) solvent system. The project aim of increasing the CF yield by using a SKP-SKL blend precursor instead of a pure SKP precursor have been met. From this work the following conclusions are made:

- It was possible to obtain dopes of SKP-SKL blends in the cold NaOH(aq) solvent system, where both SKP and SKL appeared to be dissolved and evenly distributed in the dope.
- Addition of SKL to the dopes had no effect on the dope viscosity, until what seems to be a possible breakpoint (dope C5.5 60/40 wt./wt. SKP/SKL) where a viscosity increase was observable, which may be a result of either total dope concentration or interactions between either SKP-SKL or SKP/SKL and the solvent system.
- No or very small color changes were observed in the coagulation and washing baths, suggesting that no major amount of lignin precipitation/leak occurred during the spinning process.
- PFs could be spun and collected for various SKP/SKL (wt./wt.) ratios and total dope concentrations. Continuous spinning was achieved for 15 minutes, whereafter the spinning was stopped as the dope had run out.
- The wash bath residence time had a large effect on ash content and should be further extended.
- Optimization of spinning settings depending on the dope is required to fully evaluate which mechanical properties that could be achieved.
- The PFs could successfully be converted into CFs.
- Addition of SKL to the dope increased the gravimetric conversion yield from 12 wt.% to 28 wt.% for dopes with 0 wt.% and 30 wt.% SKL respectively.
- In general, the tensile properties of the PFs and CFs decreased with increasing lignin content. For example, the TM and TS for PFs from the 5.5 wt.% SKP series decreased for 0 wt.% SKL to 30 wt.% SKL (four baths), from 1434 cN/Tex to 665 cN/Tex, and from 26 cN/Tex to 12 cN/Tex respectively, and the corresponding CFs decreased from 71 GPa to 51 GPa and from 1.17 GPa to 0.67 GPa.
- The morphology of the fibers resembled that of viscose fibers, and the CFs had a similar appearance to its PFs.

6 Future work

There are several possible future paths that seem interesting to investigate deeper regarding the concept presented in this thesis work. The evaluation of the wet spinning of SKP-SKL blends in a cold NaOH(aq) solvent system showed on possibilities, with future development and adjustment opportunities within several parts of the process. Areas of special interest are the dope preparation part as well as the wet spinning itself.

Improvements of experimental equipment:

- Extend and improve the layout of the wash baths.
- Find a solution to prevent problems with retraction of fibers on the speed-adjustable rolls during spinning.

Strive to obtain improved PFs:

- Evaluate the effect of SKP DP on spinnability and PF properties.
- Improve the dope preparation, e.g., by adjusting concentrations, optimization of the dissolution step and deaeration.
- Further evaluation of different dope concentrations.
- Optimization of spinning settings, e.g., by adjusting draw ratio, coagulation speed (concentrations and composition), wash bath parameters (such as residence time, temperature, etc.), and drying before collection.

References

[1] B. A. Newcomb, "Processing, structure, and properties of carbon fibers - review," *Composites: Part A,* no. 91, pp. 262-282, 2016.

[2] F. G. Calvo-Flores, J. A. Dobado, J. Isac-García and F. J. Martín-Martínez, "Functional and Spectroscopic Characterization of Lignins," in *Lignin and Lignans as Renewable Raw Materials - Chemistry, Technology, and Applications*, John Wiley & Sons, Incorporated, 2015, pp. 145-188.

[3] X. Huang, ”Fabrication and Properties of Carbon Fibers,” *Materials,* vol. 2, pp. 2369-2403, 2009.

[4] O. Bahl, Z. Shen, J. G. Lavin and R. A. Ross, "Manufacture of Carbon Fibers," in *Carbon fibers*, New York, Marcel Dekker Inc., 1998, pp. 1-85.

[5] A. Bengtsson, J. Bengtsson, H. Theliander, M. Ek, E. Sjöholm, T. Köhnke, M. Sedin and K. Jedvert, "LightFibre and beyond - towards the bio-based carbon fibres of the future," in *European Workshop on Lignocellulosics and Pulp*, Gothenburg, Sweden, 2022.

[6] A. Bengtsson, J. Bengtsson, C. Olsson, M. Sedin, K. Jedvert, H. Theliander and E. Sjöholm, "Improved yield of carbon fibres from cellulose and kraft lignin," *Holzforschung,* vol. 72, no. 12, p. 1007–1016, 2018.

[7] A. Bengtsson, "Carbon fibres from lignin-cellulose precursors (Licentiate Thesis)," KTH Royal Institute of Technology, Stockholm, Sweden, 2019.

[8] J. Bengtsson, "Spinning of lignin-cellulose carbon-fiber precursors (Licentiate Thesis)," Chalmers University of Technology, Gothenburg, Sweden, 2019.

[9] M. B. Jansson and N.-O. Nilvebrant, "Wood extractives," in *Wood chemistry and Wood biotechnology*, vol. 1, Berlin, De Gruyter Inc., 2009, pp. 147-172.

[10] E. Sjöström, Wood chemistry - Fundamentals an Applications (Second Edition), London: Academic Press Inc., 1993.

[11] G. Henriksson, ”Lignin,” i *Wood Chemistry and Biotechnology*, Berlin, De Gruyter , 2009, pp. 121-146.

[12] G. Henriksson, E. Brännvall and H. Lennholm, "The Trees," in *Wood Chemistry and Wood Biotechnology*, vol. 1, Berlin, De Gruyter Inc., 2009, pp. 13-44.

[13] G. Henriksson and H. Lennholm, "Cellulose and Carbohydrate Chemistry," in *Wood Chemistry and Biotechnology*, Berlin, de Gruyter, 2009, pp. 72-100.

[14] M. Gunnarsson, *Understanding overlooked molecular interactions in the cellulose/NaOH(aq) system,* Göteborg: Chalmers University of Technology, 2019.

[15] T. Liitiä, S. L. Maunu and B. Hortling, "Effects of pulping on crysstallinity of cellulose studied by solid stat NMR," in *Cellulosic pulps, fibres and materials*, Cambridge, Woodhead publishing Limited, 2000, pp. 39-44.

[16] H. Kumar and L. P. Christopher, "Recent trends and developments in dissolving pulp production and application," *Cellulose,* no. 24, pp. 2347-2365, 2017.

[17] P. Alexandridis, M. Ghasemi, E. P. Furlani and M. Tsianou, "Solvent processing of cellulose for effective bioresource utilization," *Current Opinion in Green and Sustainable Chemistry,* vol. 14, pp. 40-52, 2018.

[18] J.-L. Wertz, O. Bédué and J. P. Mercier, "Swelling and dissolution of cellulose," in *Cellulose science and technology*, EPFL Press, 2010, pp. 147-208.

[19] B. Lindman, G. Karlström and L. Stigsson, "On the mechanism of dissolution of cellulose," *Journal of Molecular Liquids,* no. 156, pp. 76-81, 2010.

[20] E. Bialik, B. Stenqvist, Y. Fang, Å. Östlund, I. Furó, B. Lindman, M. Lund and D. Bernin, "Ionization of Cellobiose in Aqueous Alkali and the Mechanism of Cellulose Dissolution," *The Journal of Physical Chemistry Letters,* no. 7, pp. 5044-5048, 2016.

[21] E. Melro, L. Alves, F. E. Antunes and B. Medronho, "A brief overview on lignin dissolution," *Journal of Molecular Liquids,* no. 265, pp. 578-584, 2018.

[22] M. Norgren and B. Lindström, "Physico-Chemical Characterization of a Fractionated Kraft Lignin," *Holzforschung,* vol. 54, no. 5, pp. 528-534, 2000.

[23] J. Sameni, S. Krigstin and M. Sain, "Solubility of lignin and acetylated lignin in organic solvents," *BioResources,* vol. 12, no. 1, pp. 1548-1565, 2017.

[24] J.-P. R. Chauvin and D. A. Pratt, "On the Reactions of Thiols, Sulfenic Acids, and Sulfinic Acids with Hydrogen Peroxide," *Angewandte Chemie International Edition ,* vol. 56, p. 6255 –6259, 2017.

[25] M. Norgren, H. Edlund and L. Wågberg, "Aggregation of lignin derivatives under alkaline conditions. Kinetics and aggregate structure," *Langmuir,* vol. 18, pp. 2859-2865, 2002.

[26] M. Norgren and H. Edlund, "Stabilisation of kraft lignin solutions by surfactant additions," *Colloids and Surfaces - A: Physicochemical and Engineering Aspects,* vol. 194, pp. 239-248, 2001.

[27] T. Budtova and P. Navard, "Cellulose in NaOH-water based solvents: a review," *Cellulose,* no. 23, pp. 5-55, 2016.

[28] M. Northolt, H. Boerstoel, H. Maatman, R. Huisman, J. Veurink and H. Elzerman, "The structure and properties of cellulose fibres spun from an anisotropic phosphoric acid solution," *Polymer,* vol. 42, no. 19, pp. 8249-8264, 2001.

[29] P. White, "Lyocell: the production process and market development," in *Regenerated cellulose fibres*, Cambridge, Woodhead Publishing Limited, 2001, pp. 62-87.

[30] A. Duval, F. Vilaplana, C. Crestini and M. Lawoko, "Solvent screening for the fractionation of industrial kraft lignin," *Holzforschung,* vol. 70, no. 1, pp. 11-20, 2016.

[31] E. C. Achinivu, R. M. Howard, G. Li, H. Graczb and W. A. Henderson, "Lignin extraction from biomass with protic ionic liquids," *Green Chemistry,* vol. 16, no. 3, pp. 1114-1119, 2014.

[32] S. Khandelwal, Y. K. Tailor and M. Kumar, "Deep eutectic solvents (DESs) as eco-friendly and sustainable solvent/catalyst systems in organic transformations," *Journal of Molecular Liquids,* vol. 215, pp. 345-386, 2016.

[33] A. Paiva, R. Craveiro, I. Aroso, M. Martins, R. L. Reis and A. R. C. Duarte, "Natural Deep Eutectic Solvents − Solvents for the 21st Century," *ACS Sustainable Chemistry & Engineering ,* vol. 2, pp. 1063-1071, 2014.

[34] M. Freemantle, An Introduction to Ionic Liquids, Cambridge: The Royal Society of Chemistry, 2010.

[35] B. Lindman, G. Karlström and L. Stigsson, "On the mechanism of dissolution of cellulose," *Journal of Molecular Liquids,* no. 156, pp. 76-81, 2010.

[36] A. M. Socha, R. Parthasarathi, J. Shi, S. Pattathil, D. Whyte, M. Bergeron, A. George, K. Tran, V. Stavila, S. Venkatachalam, M. G. Hahn, B. A. Simmons and S. Singh, "Efficient biomass pretreatment using ionic liquids derived from lignin and hemicellulose," *National Academy of Sciences,* vol. 111, no. 35, pp. E3587-E3595, 2014.

[37] D. Glas, C. Van Doorslaer, D. Depuydt, F. Liebner, T. Rosenau, K. Binnemans and D. E. De Vos, "Lignin solubility in non-imidazolium ionic liquids," *Journal of Chemical Technology & Biotechnology, October 2015, Vol.90(10), pp.1821-1826,* vol. 90, no. 10, pp. 1821-1826, 2015.

[38] M. Egal, T. Budtova and P. Navard, "Structure of Aqueous Solutions of Microcrystalline Cellulose/Sodium Hydroxide below 0 degree C and the Limit of Cellulose Dissolution," *Biomacromolecules,* vol. 8, no. 7, pp. 2282-2287, 2007.

[39] J. Mercer, "Improvements in the preparation of cotton and others fabrics and other fibrous materials". Patent British Patent 13 296, 24 October 1850.

[40] A. G. Wilkes, "The viscose process," in *Regenerated cellulose fibres*, Cambridge, Woodhead Publishing Limited, 2001, pp. 37-57.

[41] L. Lilienfeld, "Manufacture of cellulose solution". Patent British Patent 212 864, 2 October 1924.

[42] H. Sobue, H. Kiessig and K. Hess, "The cellulose–sodium hydroxide–water system as a function of the temperature," *Z Phys Chem B,* no. 43, pp. 309-328, 1939.

[43] K. Kamide, K. Okajima and K. Kowsaka, "Dissolution of Natural Cellulose into Aqueous Alkali Solution: Role of Super-Molecular Structure of Cellulose," *Polymer Journal,* vol. 24, no. 1, pp. 71-86, 1992.

[44] A. Isogai, "NMR analysis of cellulose dissolved in aqueous NaOH solutions," *Cellulose,* vol. 4, pp. 99-107, 1997.

[45] M. Egal, T. Budtova and P. Navard, "Structure of Aqueous Solutions of Microcrystalline Cellulose/Sodium Hydroxide below 0 °C and the Limit of Cellulose Dissolution," *Biomacromolecules,* no. 8, pp. 2282-2287, 2007.

[46] C. Roy, T. Budtova and O. Bedue, "Structure of Cellulose-Soda Solutions at Low Temperatures," *Biomacromolecules,* vol. 2, no. 3, pp. 687-693, 2001.

[47] J. Cai and L. Zhang, "Rapid Dissolution of Cellulose in LiOH/Urea and NaOH/Urea Aqueous Solutions," *Macromolecular Bioscience,* no. 5, pp. 539-548, 2005.

[48] Z. Jiang, Y. Fang, Y. Ma, M. Liu, R. Liu, H. Guo, A. Lu and L. Zhang, "Dissolution and Metastable Solution of Cellulose in NaOH/Thiourea at 8 °C for Construction of Nanofibers," *The Journal of Physical Chemistry B,* no. 121, pp. 1793-1801, 2017.

[49] Q. Yang, H. Qi, A. Lue, K. Hu, G. Cheng and L. Zhang, "Role of sodium zincate on cellulose dissolution in NaOH/urea aqueous solution at low temperature," *Carbohydrate Polymers,* no. 83, pp. 1185-1191, 2011.

[50] L. Yan and Z. Gao, "Dissolving of cellulose in PEG/NaOH aqueous solution," *Cellulose,* no. 15, pp. 789-796, 2008.

[51] R. Sescousse, A. Smacchia and T. Budtova, "Influence of lignin on cellulose-NaOH-water mixtures properties and on Aerocellulose morphology," *Cellulose ,* no. 17, pp. 1137-1146, 2010.

[52] D. Cienchañska and P. Nousiainen, "Cellulosic fibres and fabric processing," in *Biodegradable and sustainable fibres*, Cambridge, Woodhead Publishing Limited, 2005, pp. 111-156.

[53] D. Edie, "The effect of processing on the structure and properties of carbon fibers," *Carbon (UK),* vol. 36, no. 4, pp. 345-362, 1998.

[54] L. Qiu, X. Zheng, J. Zhu, G. Su and D. Tang, "The effect of grain size on the lattice thermal conductivity of an individual polyacrylonitrile-based carbon fiber," *Carbon,* vol. 51, pp. 265-273, 2013.

[55] SGL Carbon Group, "Composite Oracle Database," [Online]. Available: http://www.composite-oracle.com/main.asp?redir2=%2Fmaterials.asp&idn=2&mainq=3&vq=q. [Accessed 26 May 2020].

[56] Sohim, "OJSC «SvetlogorskKhimvolokno»," [Online]. Available: http://www.sohim.by/en/produktsiya/uglerodnye-materialy/volokna/. [Accessed 26 May 2020].

[57] P. Morgan, "History and Early Development of Carbon Fibers," in *Carbon Fibers and Their Composites*, Boca Raton, CRC Press, 2005, pp. 65-120.

[58] Sohim, "Rayon Based Carbon Fibres," Khimvolokno, [Online]. Available: http://www.sohim.by/en/produktsiya/uglerodnye-materialy/volokna/. [Accessed 26 May 2020].

[59] C. Vasile, A. Grigoriu and V. Blascu, "Particulate Fillers and Fibre Reinforcements," in *Handbook of Polymer Blends and Composites*, United Kingdom, Rapra Technology Ltd., 2002, pp. 39-78.

[60] W. Qu, Y. Xue, Y. Gao, M. Rover and X. Bai, "Repolymerization of pyrolytic lignin for producing carbon fiber with improved properties," *Biomass and Bioenergy,* vol. 95, pp. 19-26, 2016.

[61] D. A. Baker and T. G. Rials, "Recent Advances in Low-Cost Carbon Fiber Manufacture from Lignin," *Journal of Applied Polymer Science,* pp. 713-728, 2013.

[62] E. Brännvall and K. Walter, "Process modifcations to obtain a prehydrolysis kraft dissolving pulp with low limiting pulp viscosity," *Nordic Pulp & Paper Research Journal,* vol. 35, no. 3, p. 332–341, 2020.

[63] S.-E. Mörtstedt and G. Hellsten, Data och diagram - Energi- och kemitekniska tabeller, Sweden: Almqvist & Wiksell Läromedel AB, 1994.

[64] F. Aldaeus, A.-M. Olsson and J. Stevanic, "Miniaturized determination of ash content in kraft lignin samples using oxidative thermogravimetric analysis," *Nordic Pulp & Paper Research Journal,* no. 32, pp. 280-282, 2017.

[65] M. Vehviläinen, ”Wet-Spinning of Cellulosic Fibres from Water-Based Solution Prepared from Enzyme-Treated Pulp (Thesis for the degree of Doctor of Science in Technology),” Tampere University of Technology , Tampere, 2015.

[66] W. Liu, T. Budtova and P. Navard, "Influence of ZnO on the properties of dilute and semi-dilute cellulose-NaOH-water solutions," *Cellulose,* no. 18, pp. 911-920, 2011.

[67] P. Morgan, "Carbon Fiber Production using a Cellulosic based Precursor," in *Carbon Fibers and Their Composites*, Boca Raton, CRC Press, 2005, pp. 269-294.

[68] A. Hirons and P. Thomas, "Tree nutrition," in *Applied tree biology*, John Wiley & Sons, Incorporated, 2018, pp. 420-442.

[69] J. Thomas and T. Gemming, "Let us use the analytical possibilities," in *Analytical transmission electron microscopy: An introduction for operators*, Springer Science & Business, 2014, pp. 177-226.

[70] D. E. Newbury, "Mistakes Encountered During Automatic Peak Identification of Minor and Trace Constituents in Electron-Excited Energy Dispersive X-Ray Microanalysis," *Scanning,* vol. 31, pp. 91-101, 2009.

[71] P. J. Statham, "Limitations to Accuracy in Extracting Characteristic Line Intensities From X-Ray Spectra," *Journal of Research of the National Institute of Standards and Technology,* vol. 107, no. 6, p. 531–546, 2002.

[72] H. Sixta, A. Michud, L. Hauru, S. Asaadi, Y. Ma, A. W. King, I. Kilpeläinen and a. M. Hummel, "Ioncell-F: A High-strength regenerated cellulose fibre," *Nordic Pulp & Paper Research Journal,* vol. 30, no. 1, pp. 43-57, 2015.

[73] Q. Liu, C. Lv, Y. Yang, F. He and L. Ling, "Study on the pyrolysis of wood-derived rayon fiber bythermogravimetry – mass spectrometry," *Journal of Molecular Structure,* no. 733, pp. 193-202, 2005.

[74] A. Bengtsson, J. Bengtsson, M. Sedin and E. Sjöholm, "Carbon Fibers from Lignin-Cellulose Precursors: Effect of Stabilization Conditions," *ACS Sustainable Chemistry & Engineering,* no. 7, pp. 8440-8448, 2019.

[75] W. Roberts, "The high temperature reactions sodium sulfate and carbon monoxide," Oklahoma Agricultural and Mechanical Collage, Stillwater, Oklahoma, 1945.

[76] "American elements," [Online]. Available: https://www.americanelements.com/zinc-sulfate-7733-02-0. [Accessed 28 October 2022].

[77] N. Byrne, R. D. Silva, Y. Ma, H. Sixta and M. Hummel, "Enhanced stabilization of cellulose-lignin hybrid filaments for carbon fiber production," *Cellulose,* vol. 25, pp. 723-733, 2018.

[78] N.-D. Le, M. Trogen, R. J. Varley, M. Hummel and N. Byrne, "Chemically Accelerated Stabilization of a Cellulose−Lignin Precursor as a Route to High Yield Carbon Fiber Production," *Biomacromolecules,* vol. 23, pp. 839-846, 2022.

[79] A. G. Dumanlı and A. H. Windle, "Carbon fibres from cellulosic precursors: a review," *Journal of Material Science,* vol. 47, no. 10, pp. 4236-4250, 2012.

[80] I. Brodin, M. Ernstsson, G. Gellerstedt and E. Sjöholm, "Oxidative stabilisation of kraft lignin for carbon fibre production," *Holzforschung ,* vol. 66, pp. 141-147, 2012.

[81] A. Bengtsson, P. Hecht, J. Sommertune, M. Ek, M. Sedin and E. Sjöholm, "Carbon Fibers from Lignin−Cellulose Precursors: Effect of Carbonization Conditions," *ACS Sustainable Chemistry & Engineering,* no. 8, pp. 6826-6833, 2020.

Appendix 1 – Spinning dopes

There was a total of eight different dopes with six different SKP/SKL ratios which were evaluated within the study as well as the estimated viscosity of each dope, retrieved through Eq. 5. (section 3.5.2), can be found in Tab. 8. The baseline (dope solvent+SKL) had a viscosity of 1.1×10^{-6} m^2s.

Table 8. Dope composition, SKP and SKL, and viscosity.

Dope	SKP (wt.%)	SKL (wt.%)	SKP/SKL (wt./wt.)	Total dope conc. (wt.%)	$\mu_{Dope}/\rho_{Dope}\times10^4$ (m^2s)
C4.5-L0	4.5	0.0	100/0	4.5	1.6
C4.5-L30	4.5	1.9	70/30	6.4	1.6
C4.5-L35	4.5	2.4	65/35	6.9	1.2
C5.5-L0	5.5	0.0	100/0	5.5	4.3
C5.5-L10	5.5	0.6	90/10	6.1	4.2
C5.5-L20	5.5	1.4	80/20	6.9	3.8
C5.5-L30	5.5	2.4	70/30	7.9	4.6
C5.5-L40	5.5	3.7	60/40	9.2	7.8

Appendix 2 – Spinning settings

The theoretical values of draw ratio, stretch ratio and total draw ratio are presented in Tab. 9, while actual values are presented in Tab. 10 together with retrieved linear density of the PFs.

Table 9. Theoretical draw ratio, stretch ratio, and total draw ratio for PF spinning with two and four wash baths respectively.

Number of wash baths used	Draw ratio	Stretch ratio	Total draw ratio
2	1.8	1.2	2.2
4	1.8	1.3	2.4

Table 10. Actual draw ratio (over section C), stretch ratio (over section W1 to D), and total draw ratio achieved during spinning trials, and the attained linear density (dTex) of PFs.

Sample	Draw ratio	Stretch ratio	Total draw ratio	Linear density (dTex)
C4.5-L0-B2	N/A	N/A	N/A	N/A
C4.5-L30-F-B2	N/A	N/A	N/A	N/A
C4.5-L35-F-B2	0.8	1.2	1.0	7.3
C4.5-L0-B4	N/A	N/A	N/A	N/A
C4.5-L30-F-B4	N/A	N/A	N/A	N/A
C4.5-L35-F-B4	0.9	1.3	1.3	5.5
C5.5-L0-B2	1.5	1.2	1.9	3.2
C5.5-L10-B2	0.5	1.2	0.6	9.6
C5.5-L20-B2	0.5	1.2	0.7	7.2
C5.5-L30-B2	0.7	1.2	0.9	7.4
C5.5-L30-F-B2	0.8	1.2	1.0	6.9
C5.5-L40-F-B2	1.0	1.2	1.2	9.1
C5.5-L0-B4	1.7	1.3	2.2	2.0
C5.5-L10-B4	1.2	1.3	1.7	2.8
C5.5-L20-B4	0.5	1.3	0.6	9.5
C5.5-L30-B4	0.6	1.3	0.8	6.8
C5-5-L30-F-B4	0.9	1.3	1.2	5.8

Appendix 3 – Ash content of precursor fibers

The ash content and ash composition of PFs obtained within the project spinning trials are presented in Tab. 11.

Table 11. Ash content supplemented with main ash composition for no and high SKL content of PFs.

Sample	Ash content (wt.%)	Ash composition (wt.%)			
		O	Na	S	Zn
C4.5-L0-B2	23.9 (1.2)	37.7 (2.5)	24.0 (4.5)	18.2 (4.7)	1.0 (0.7)
C4.5-L30-F-B2	22.2 (0.5)	N/A	N/A	N/A	N/A
C4.5-L35-F-B2	9.9 (0.0)	33.6 (3.8)	16.3 (4.8)	11.3 (3.7)	1.1 (0.4)
C4.5-L0-B4	3.3 (0.4)	36.9 (1.9)	21.9 (3.1)	15.2 (5.8)	1.3 (0.4)
C4.5-L30-F-B4	4.8 (0.3)	N/A	N/A	N/A	N/A
C4.5-L35-F-B4	3.7 (0.2)	40.4 (3.3)	26.4 (6.1)	16.6 (4.4)	1.9 (0.4)
C5.5-L0-B2	11.9 (0.2)	27.3 (3.7)	12.3 (4.1)	8.3 (4.3)	0.6 (0.2)
C5.5-L10-B2	7.1 (0.0)	N/A	N/A	N/A	N/A
C5.5-L20-B2	4.5 (0.0)	N/A	N/A	N/A	N/A
C5.5-L30-B2	6.7 (0.6)	41.2 (1.8)	26.7 (1.8)	18.2 (1.7)	1.9 (0.2)
C5.5-L30-F-B2	7.1 (0.4)	N/A	N/A	N/A	N/A
C5.5-L40-F-B2	14.3 (1.3)	N/A	N/A	N/A	N/A
C5.5-L0-B4	0.6 (0.3)	40.6 (1.8)	26.5 (4.5)	16.6 (3.9)	2.7 (0.4)
C5.5-L10-B4	0.5 (0.0)	N/A	N/A	N/A	N/A
C5.5-L20-B4	1.9 (0.2)	N/A	N/A	N/A	N/A
C5.5-L30-B4	1.3 (0.4)	40.0 (1.3)	22.9 (0.8)	12.3 (1.5)	1.7 (0.2)
C5.5-L30-F-B4	4.6 (0.1)	N/A	N/A	N/A	N/A

Appendix 4 – Mechanical properties of precursor fibers

The reported values from the single fiber tensile testing of PFs in Tab. 12 is an average of 30–35 individual measurements.

Table 12. Single fiber tensile testing results of PFs.

Sample	dTex	TS (cN/Tex)	TM (cN/Tex)	Strain at break (%)
C4.5-L0-B2	N/A	N/A	N/A	N/A
C4.5-L30-F-B2	N/A	N/A	N/A	N/A
C4.5-L35-F-B2	7.3	6.4 (0.9)	407 (41)	2.3 (0.8)
C4.5-L0-B4	N/A	N/A	N/A	N/A
C4.5-L30-F-B4	N/A	N/A	N/A	N/A
C4.5-L35-F-B4	5.5	11.1 (2.0)	672 (123)	3.2 (0.8)
C5.5-L0-B2	3.2	19 (1.5)	1199 (53)	4.2 (1.1)
C5.5-L10-B2	9.6	20 (1.3)	1375 (84)	5.7 (1.3)
C5.5-L20-B2	7.2	18 (1.3)	1123 (57)	3.6 (0.9)
C5.5-L30-B2	7.4	12 (1.1)	749 (69)	3.0 (0.8)
C5.5-L30-F-B2	6.9	13 (1.1)	839 (78)	2.8 (0.5)
C5.5-L40-F-B2	9.1	7 (0.6)	524 (52)	1.7 (0.6)
C5.5-L0-B4	2.0	27 (1.1)	1450 (135)	4.9 (0.6)
C5.5-L10-B4	2.8	22 (1.5)	1180 (98)	4.8 (1.0)
C5.5-L20-B4	9.5	14 (0.8)	818 (47)	5.7 (1.6)
C5.5-L30-B4	6.8	12 (0.9)	665 (43)	6.6 (1.9)
C5.5-L30-F-B4	5.8	12 (0.8)	734 (51)	3.6 (0.7)

TS = Tensile strength, TM = Tensile modulus

Fig. 22 shows the TS and TM against the total dope concentration of the dope used to wet spin the PFs.

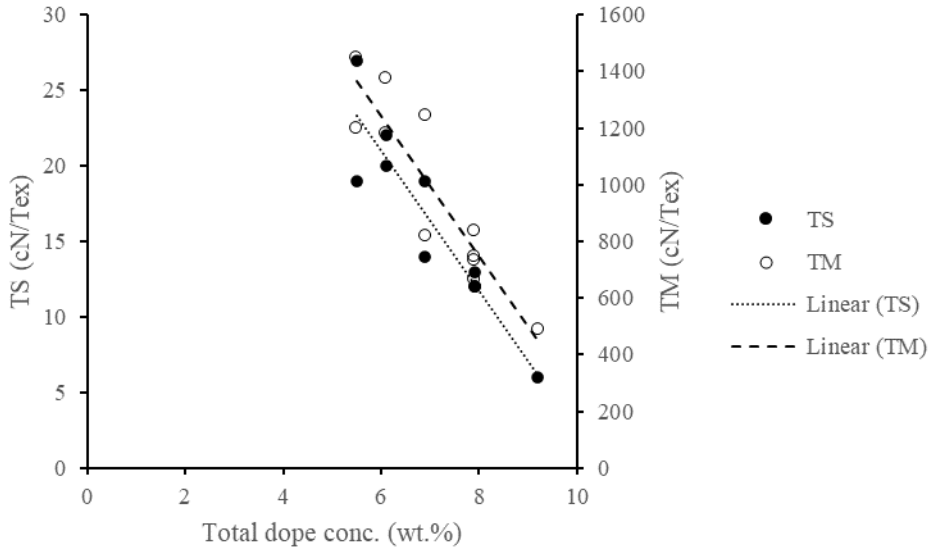

Figure 22. TS and TM of PFs from the C5.5 dope series in correlation to the total dope concentration of the dope used to spin the PFs.

In Fig. 23 TS and TM are depicted against the linear density (dTex). However, it should be noted that three fibers (C5.5-L10-B2, C5.5-L20-B2, and C5.5-L20-B4) have values which are off compared to both the TS and TM trend, and these are therefor not included in the diagram below. The reason for the deviation is most likely a human error when counting the fibers for the dTex calculations.

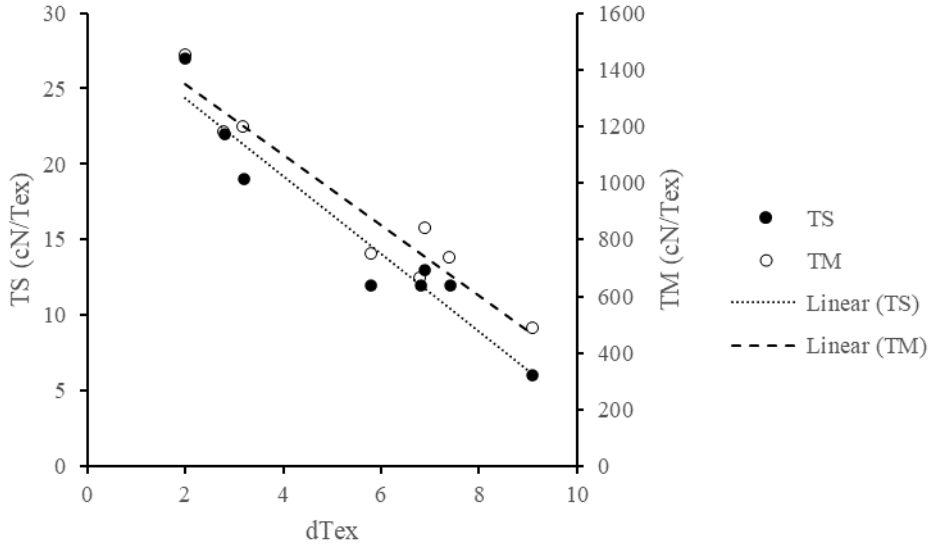

Figure 23. The TS and TM of PFs from the C5.5 dope series in correlation to the linear density (dTex) of the fibers.

In Fig. 24 the strain at break is depicted against ash content of the PF.

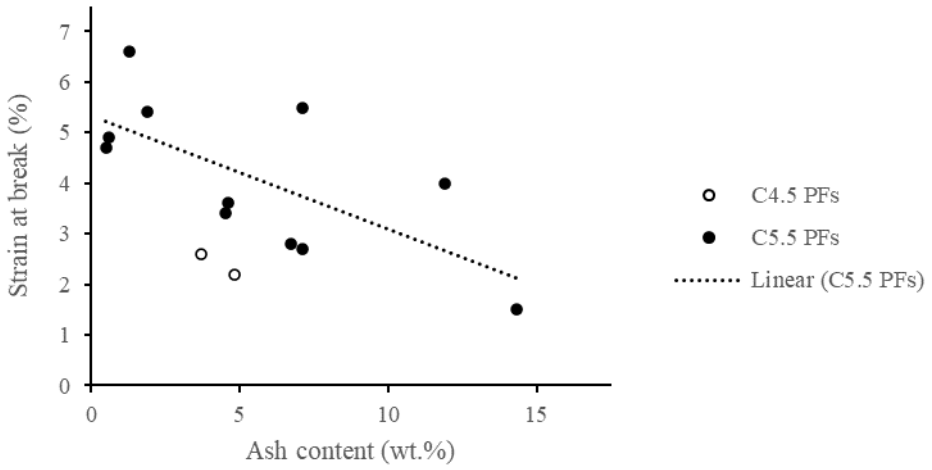

Figure 24. Correlation between strain at break and ash content of PFs.

Appendix 5 – Pyrolysis yield of precursor fibers

Theoretical and measured pyrolysis yield, obtained through analysis described in section 3.5.4, as well as relative pyrolysis yield of the PFs, are found in Tab. 13.

Table 13. Pyrolysis yield obtained via TGA analysis.

Sample	Pyrolysis yield (wt.%)	Theoretical yield (wt.%)	Relative yield (%)
C4.5-L0-B2	18.5 (0.1)	44.4	41.7
C4.5-L30-F-B2	26.8 (0.1)	50.3	53.3
C4.5-L35-F-B2	26.6 (0.2)	51.3	51.9
C4.5-L0-B4	15.1 (1.3)	44.4	34.0
C4.5-L30-F-B4	13.8 (1.4)	50.3	27.4
C4.5-L35-F-B4	16.9 (0.9)	51.3	32.9
C5.5-L0-B2	17.1 (0.2)	44.4	38.5
C5.5-L10-B2	20.8 (1.4)	46.4	44.8
C5.5-L20-B2	15.8 (0.6)	48.3	32.7
C5.5-L30-B2	15.0 (1.0)	50.3	29.8
C5.5-L30-F-B2	22.7 (0.6)	50.3	45.1
C5.5-L40-F-B2	26.3 (0.2)	52.2	50.4
C5.5-L0-B4	5.3 (0.1)	44.4	11.9
C5.5-L10-B4	7.6 (0.2)	46.4	16.4
C5.5-L20-B4	11.9 (1.4)	48.3	24.6
C5.5-L30-B4	11.6 (0.3)	50.3	23.1
C5.5-L30-F-B4	13.2 (0.2)	50.3	26.2